博士論文

Specific impairment of the late phase of climbing fiber synapse elimination by global scaling-down of excitatory postsynaptic responses in cerebellar Purkinje cells

（小脳プルキンエ細胞の興奮性シナプス応答の全般的減少による登上線維シナプス除去の後期過程特異的な障害）

川田　慎也

CONTENTS

ABSTRACT

Developmental synapse elimination is crucial for precise formation of mature neural circuits. While relative differences in synaptic strengths among competing inputs are essential for synapse elimination, it is unclear how absolute strengths of synaptic inputs influence developmental synapse elimination. Here we addressed this question using cerebellar climbing fiber (CF)-Purkinje Cell (PC) synapse elimination as a model system. We generated mice with PC-selective deletion of stargazin (TARP γ-2), the major AMPA receptor auxiliary subunit in PCs (γ-2 PC-KO). While relative differences in the amplitudes of "strong" and "weak" CF-mediated postsynaptic responses were preserved, the absolute strengths of CF synaptic inputs to PCs were scaled down globally in whole PCs of γ-2 PC-KO mice at P6 and thereafter. Dendritic CF translocation, which normally starts at P9, was moderately impaired but the early phase of CF synapse elimination, which normally proceeds from P7 to P11, was apparently normal in γ-2 PC-KO mice. In contrast, the degree of multiple CF innervation of PCs was significantly higher in γ-2 PC-KO mice than in wild-type mice at P15-P17 and P21-P43. CF-induced Ca^{2+} transients in

PC dendrites were markedly reduced in γ-2 PC-KO mice. Importantly, lentivirus-mediated overexpression of *Arc* into PCs rescued the impaired CF synapse elimination in γ-2 PC-KO mice. These results indicate that the late phase of CF synapse elimination, which normally proceeds from P12 to P17 and involves Ca^{2+}-dependent *Arc* activation in PCs, is impaired in γ-2 PC-KO mice. We conclude that proper synaptic scaling is an important factor for developmental CF synapse elimination.

INTRODUCTION

Proper function of the nervous system is critically dependent on precise formation of neural circuits during development. In developing nervous system, redundant synaptic connections are formed initially around birth. Then, functionally important synapses are strengthened and unnecessary redundant connections are eliminated during subsequent postnatal period (Hensch, 2004; Katz and Shatz, 1996; Lichtman and Colman, 2000; Purves and Lichtman, 1980). This process, known as synapse elimination, is widely thought to be crucial for shaping mature functional neural circuits in activity-dependent manners in various regions of the central and peripheral nervous systems (Kano and Hashimoto, 2009; Lichtman and Colman, 2000; Purves and Lichtman, 1980) and in various animal species from *Caenorhabditis elegans* to human (Luo and O'Leary, 2005). It is widely thought that functional changes in synaptic strength precede morphological alterations in synaptic connection (Kano and Hashimoto, 2009). Immature synapses are thought to be selectively strengthened or weakened before they are structurally stabilized or eliminated. Functional changes are thought to depend on Hebbian type synaptic

plasticity in which long-term potentiation (LTP) or depression (LTD) is induced in synapse-specific and activity-dependent manners (Hayama et al., 2013; Matsuzaki et al., 2004). Synaptic strength is also dependent on homeostatic plasticity, which globally scales synaptic strengths in whole neurons up or down against neural activity in a synapse-nonspecific manner (Turrigiano, 2012; Turrigiano, 2008). Homeostatic plasticity does not change the relative differences in synaptic strengths of competing inputs in individual neurons (Turrigiano, 2012; Turrigiano, 2008). It is however unclear whether global changes in synaptic strengths in individual neurons affect developmental synapse elimination.

In the present study, we addressed this question using developmental synapse elimination at cerebellar climbing fiber (CF)-Purkinje Cell (PC) synapse as a model (Hashimoto and Kano, 2013; Watanabe and Kano, 2011). In the cerebellum of neonatal rodents, the soma of PCs is innervated by >5 CFs with similar synaptic strengths (Hashimoto and Kano, 2003). A single CF input is selectively strengthened among multiple CF inputs to each PC from Postnatal day 3 (P3) to P7 (the phase of "functional

differentiation") (Hashimoto and Kano, 2003; Kawamura et al., 2013). Then, only the strengthened CF (the "winner" CF) extends its innervation along growing PC dendrites from P9 (Carrillo et al., 2013; Hashimoto et al., 2009; Ichikawa et al., 2011). In parallel, synapses of the other weaker CFs ("loser" CFs) left on the PC soma are eliminated depending on two distinct mechanisms from P7 to P11 (the "early phase") and from P12 to P16 (the "late phase") (Hashimoto and Kano, 2013; Watanabe and Kano, 2011). It has been demonstrated that LTP and LTD occur at CF-PC synapses during the first postnatal week in acute cerebellar slices from rats (Bosman et al., 2008) and mice (Ohtsuki and Hirano, 2008). Using in vivo whole-cell recordings from PCs in living rats and mice, we have recently reported that the selective strengthening of single CFs in the first postnatal week appears to dependent on spike-timing dependent plasticity (Kawamura et al., 2013), a Hebbian type synaptic plasticity widely believed to underlie synapse refinement in developing brain (Holtmaat and Svoboda, 2009). Furthermore, LTD at CF-PC synapses is reported to occur during the third postnatal week in a manner dependent on type 1 metabotropic glutamate receptor (mGluR1) (Hansel and Linden, 2000). These results

suggest that Hebbian type synaptic plasticity underlies postnatal development of CF-PC synapses and that relative differences in synaptic strengths between CF inputs to individual PCs are important for CF synapse elimination. In contrast, it is totally unknown whether global changes in synapse strengths in whole PCs affect CF synapse elimination.

In order to reduce excitatory synaptic strengths globally in PCs during postnatal development, we generated mice with PC-selective deletion of stargazin (TARP γ-2), a major AMPA receptor auxiliary subunit that regulates surface expression of AMPAR (Hashimoto et al., 1999; Jackson and Nicoll, 2011). Similarly to the previous results from mice with global deletion of TARP γ-2 (Menuz and Nicoll, 2008; Yamazaki et al., 2010), the absolute amplitude of CF-mediated EPSCs (CF-EPSCs) of our PC-selective TARP γ-2 knockout mice (γ-2 PC-KO mice) was about half of wild-type mice. Importantly, in γ-2 PC-KO mice, the reduction of CF-EPSC amplitude was not observed from P3 to P5 but became obvious at P6 and thereafter. Because of this developmental profile, functional differentiation of multiple CF inputs, which proceeds from P3 to P7, was normal in γ-2 PC-KO mice. Thus γ-2 PC-KO mice after P7 provided a good model in which relative

differences in synaptic strengths between winner and loser CFs are normal but absolute amplitudes of CF-EPSCs are globally scaled down to about half in whole PCs. Using this mouse model, we investigated whether and how global scaling down of CF synaptic strength affects the dendritic translocation of winner CFs, the early phase and the late phase of CF synapse elimination.

METHODS

Animals

All procedures for animal care and experiments were made in accordance with the guidelines of the animal welfare committees of the University of Tokyo, Hokkaido University, and Niigata University. To generate PC-specific γ-2 KO mice, we crossed the γ-2 floxed mice (γ-$2^{lox/lox}$) (Yamazaki et al., 2010) with D2CreN line (GluD$2^{+/Cre}$) (Yamasaki et al., 2011) in which Cre recombinase was expressed only in GluD2-expressing cells. γ-$2^{lox/lox}$ mice and GluD$2^{+/Cre}$ mice were produced by homologous recombination using the C57BL/6N ES cell line RENKA (Mishina and Sakimura, 2007). Detailed procedures are described in previous reports (Yamasaki et al., 2011; Yamazaki et al., 2010). For each experiment, male mice (γ-$2^{lox/lox}$, GluD$2^{+/Cre}$) and female mice (γ-$2^{lox/lox}$, GluD$2^{+/+}$) were crossed to obtain control (γ-$2^{lox/lox}$, GluD$2^{+/+}$) and PC-selective γ-2 knockout (γ-$2^{lox/lox}$, GluD$2^{+/Cre}$, γ-2 PC-KO) mice.

Electrophysiology

Mice at P3-P43 were decapitated under CO_2 anesthesia and their brains were quickly removed. After trimming, the brains were placed in cooled ACSF (0-4 °C) containing (in mM) 125 NaCl, 2.5 KCl, 2 $CaCl_2$, 1 $MgSO_4$, 1.25 NaH_2PO_4, 26 $NaHCO_3$, and 20 glucose, bubbled with 95% O_2 and 5% CO_2 (pH 7.3). Parasagittal cerebellar slices (250 μm) were prepared using a vibratome slicer (VT-1200S, Leica, Germany) (Aiba et al., 1994; Kano et al., 1995). After 1hr of recovery in an incubation chamber filled with the ACSF at room temperature, a slice was moved to a recording chamber in which fresh ACSF was perfused continuously. Whole-cell patch clamp recordings were made from visually-identified PCs by using an upright microscope (Axioskop, Zeiss, Germany, or BX51W1, Olympus, Japan). Patch pipettes (2-4 MΩ) were filled with one of the internal solutions with the following compositions (in mM); 60 CsCl, 10 D-gluconate, 20 TEA-Cl, 20 BAPTA, 4 $MgCl_2$, 4 ATP, 0.4 GTP, and 30 HEPES (pH 7.3, adjusted with CsOH) for recording CF-, PF-EPSCs and mIPSCs, the same compositions plus 0.1 spermine for the measurement of exogenous AMPA-mediated current (Yamazaki et al., 2010); 65 K-D-gluconate, 65

Cs-methanesulfonate, 10 KCl, 1 $MgCl_2$, 4 Na_2ATP, 1 NaGTP, 20 Hepes, 0.4 EGTA and 5 sucrose (pH 7.3, adjusted with CsOH) for recording mGluR1-mediated currents (Mitsumura et al., 2011). The standard ACSF with the aforementioned compositions was used for recording synaptic and membrane currents with addition of the following compound(s): picrotoxin (100 μM) for recording CF-EPSCs and PF-EPSCs; cyclothiazide (100 μM) and tetrodotoxin (0.5 μM) for recording AMPA receptor-mediated membrane currents; NBQX (10 μM), R-CPP (5 μM) and tetrodotoxin (0.5 μM) for recording mIPSCs. Stimulation pipettes were filled with the ACSF and placed in the granule cell layer for evoking CF-ESPCs or in the molecular layer for evoking PF-EPSCs. Square pulses were applied for focal stimulation (duration of 100 μs, amplitude of 0 V to 100 V). The number of CFs innervating each PC was estimated by the number of discrete CF-EPSC steps (Kano et al., 1995). For recording mGluR1-mediated currents, a tungsten electrode was placed in outer half of the molecular layer. All electrophysiological recordings were performed at 32 °C except mGluR1-mediated current recording which was performed at room temperature. Ionic currents were recorded with an EPC9 patch

clamp amplifier (HEKA). Liquid junction potential was corrected. Online data acquisition and offline data analysis were performed using PULSE and PULSE Fit software (HEKA) or Mini analysis Program (ver. 6.0.1, Synaptosoft Inc.).

Ca^{2+} imaging

Recording pipettes (2-4 MΩ) were filled with either of the following internal solutions containing (in mM); 130 Cs-methanesulfonate, 5 TEA-Cl, 4 Mg-ATP, 0.3 Na_3-GTP, 10 HEPES, 1 EGTA, 1 QX314-Cl, 10 Na_2-phosphocreatine (pH 7.3, adjusted with CsOH) and 0.1 Oregon Green 488 BAPTA1 (OGB-1, Molecular Probes), which was used for imaging depolarization-induced Ca^{2+} signals (Nakayama et al., 2012); 135 K-gluconate, 10 Na-gluconate, 5 KCl, 0.5 EGTA, 10 HEPES, 4 Mg-ATP, 0.4 Na_3-GTP (pH 7.3, adjusted with NaOH) and 0.1 Oregon Green 488 BAPTA1, which was used for imaging CF-induced Ca^{2+} signals. After establishing whole-cell recording configurations, PCs were loaded for at least 25 min with the Ca^{2+} indicator OGB-1. For recording Ca^{2+} transients induced by depolarization of PCs, fluorescence images were acquired at 4 Hz

by using a confocal laser scanning microscope (Fluoview, Olympus) before and after application of a 1 s depolarizing pulse from -80mV to -10 mV to the recorded PCs. The extracellular solution was supplemented with tetrodotoxin (0.5 μM), NBQX (10 μM), picrotoxin (100 μM) and cytochrome C (0.1 mg/ml). To block P/Q-type voltage-dependent Ca^{2+} channel (VDCC), ω-agatoxin IVA (0.4 μM) was added. For recording Ca^{2+} transients induced by CF stimulation, fluorescence images were acquired at 30 Hz by using a high-speed confocal laser scanning microscope (CSU22, Yokogawa). The Ca^{2+} signals were obtained from somata or dendritic regions of PCs. The Ca^{2+}-dependent fluorescence signals from selected regions of interest (ROI) were background subtracted and expressed as increases in fluorescence divided by the prestimulus fluorescence values ($\Delta F/F_0$) using ImageJ (http://rsb.info.nih.gov/ij/). Ca^{2+} imaging was performed at 32 °C for CF-induced Ca^{2+} transients or at room temperature for depolarization-induced Ca^{2+} transients.

Immunohistochemistry

Under deep pentobarbital anesthesia (100 μg/g of body weight, i.p.), mice were perfused with 4% paraformaldehyde (PFA) in 0.1 M sodium phosphate buffer, pH 7.2, and processed for parasagittal microslicer sections (50 μm in thickness; VT1000S; Leica, Nussloch, Germany). The sections were incubated overnight with affinity-purified primary antibodies raised against the following molecules (host species, final concentration): anti-calbindin (goat, 1 μg/ml) (Miura et al., 2006), anti-parvalbumin (guinea pig, 1 μg/ml) (Miura et al., 2006), anti-VGAT (rabbit, 1 μg/ml) (Miura et al., 2006), anti-mGluR1 (rabbit, 1 μg/ml) (Tanaka et al., 2000), anti-Gαq (rabbit, 1 μg/ml) (Santa Cruz biotechnology, Santa Cruz, CA), anti-PKCγ (goat, 1 μg/ml) (Yoshida et al., 2006) and anti-PLCβ4 (guinea pig, 1 μg/ml) (Nakamura et al., 2004). Sections were incubated subsequently with a mixture of species-specific labeled secondary antibodies for 2hr (1:200 Jackson ImmunoResearch, West Grove, PA).

For immunohistochemistry of γ-2, GluA1, GluA2, GluA3 and GluA4, paraffin sections (4 μm in thickness) were made using a sliding microtome (SM1000R; Leica, Nussloch,

Germany). These sections were first subjected to pepsin pretreatment for antigen exposure, i.e., incubation in 1 mg/ml of pepsin (DAKO, Carpinteria, CA, USA) in 0.2 N HCl for 10 min at 37 °C. Then sections were incubated successively with 10% normal donkey serum for 20 min, primary antibodies against γ-2 (rabbit, 1 μg/ml), GluA1 (rabbit, 1 μg/ml), GluA2 (rabbit, 1 μg/ml), GluA3 (rabbit, 1 μg/ml) and GluA4 (guinea pig, 1 μg/ml) (Yamazaki et al., 2010) overnight, biotinylated secondart antibodies for 2 hr and avidin-biotin-peroxidase complex for 1 hr, using a Histofine SAB-PO(R) kit (Nichirei Corp., Tokyo, Japan). Immunoreaction was visualized using the tyramide signal amplification kit (Perkin-Elmer, Boston, MA, USA).

Morphological analysis of CF innervation

Combined VGluT2 immunostaining and labeling of subsets of CFs with an anterograde tracer was performed to investigate CF innervations patterns (Miyazaki and Watanabe, 2011). Under anesthesia with chloral hydrate (350mg/kg of body weight, i.p.), a glass pipette filled with 2-3 μl of 10% solution of DTR (3,000 molecular weight; Invitrogen,

Carlsbad, CA) in PBS (pH 7.4) was inserted stereotaxically to the inferior olive. The tracer was injected by air pressure at 10 psi with 5 s intervals for 1 min. After 4 days of survival, mice were perfused with 4% paraformaldehyde and fixed parasagittal cerebellar sections were made as described above. The DTR-labeled sections were incubated overnight with a mixture of goat calbindin antibody and guinea pig type II VGluT2 antibody (Miyazaki et al., 2003) followed by 2 hr incubation with a mixture of Alexa 488- (Invitrogen) and Cy5-labeled species-specific secondary antibodies. Images of triple fluorescence labeling were taken with confocal laser-scanning microscope (FV1000, Olympus).

Preparation of viral vector constructs

VSV-G pseudotyped lentiviral vectors (pCL20c) (Hanawa et al., 2002) were used in this study. The vectors were designed to express only EGFP, or EGFP and Arc or miRNA directed against Arc under the control of a truncated L7 promoter (pCL20c-trL7) (Mikuni et al., 2013; Sawada et al., 2010).

Virus preparation and injection

All procedures were done as described previously (Mikuni et al., 2013). Briefly, virus vector was produced by cotransfection of HEK293T cells with packaging plasmids and lentiviral vector using a calcium phosphate precipitation method (Torashima et al., 2006). Virus containing medium was filtered and centrifuged at 27,000 rpm for 90 min. Virus solution was injected to γ-2 PC-KO mice at P1-5 by the following procedures. Under isoflurane anesthesia, the tip of a 33-gauge Hamilton syringe attached to a micropump (UltramicroPump II; World Precision Instruments (WPI)) was placed on the exposed surface of the cerebellar vermis. 3.5 μl of viral solution was injected at a rate of 180 nl/min using a microprocessor-based controller (Micro 4; WPI).

Data analysis

To estimate the relative difference of synaptic strengths among competing inputs, we calculated the disparity ratio from each multiply-innervated PC (Hashimoto and Kano, 2003). Briefly, the amplitudes of individual CF-EPSCs in a given multiply innervated PC

were measured and they were numbered in the order of their amplitudes (A_1, A_2,…A_N, N ≧2, A_N represents the largest CF-EPSC).

$$\text{Disparity ratio} = (A_1/A_N + A_2/A_N + \ldots + A_{N-1}/A_N) / (N-1)$$

If all amplitudes in PCs were equal, disparity ratio would be 1. On the other hand, if the difference between the largest CF-EPSC amplitude and others become larger, disparity ratio becomes smaller.

Statistical analysis

All data were expressed as mean ± SEM. When two groups were compared, Wilcoxon-test was used by JMP Pro9 (SAS Institute Inc.). Two-way analysis of variance (ANOVA) with Tukey's post-hoc analysis was used for multiple comparison (**Figure 3B-3D**). When p value was less than 0.05, the difference between groups were judged to be significant.

RESULTS

Reduced AMPA receptor-mediated membrane currents and excitatory postsynaptic currents in PCs of PC-selective γ-2 knockout mice

To generate PC-selective TARP γ-2 knockout mice (γ-2 PC-KO mice), we crossed the γ-2 floxed mice (Yamazaki et al., 2010) with D2CreN mice ($GluD2^{+/Cre}$) in which Cre recombinase is expressed under the control of the GluD2 promoter (Hashimoto et al., 2011; Nakayama et al., 2012). While γ-2 global knockout mice (γ-2 KO) show ataxic gait and head-lifting behavior, and are smaller in size than wild-type mice, γ-2 PC-KO mice are viable, fertile and apparently indistinguishable from their wild-type littermates. Immunohistochemical analysis revealed that, in γ-2 PC-KO mice at postnatal day 21 (P21), γ-2 signal was greatly reduced in the molecular layer (ML) but was normal in the granule cell layer (GCL) of the cerebellum (**Figures 1A and 1B**). As a consequence of the reduction of γ-2, immunoreactivity for AMPA receptor GluA2 and GluA3 subunits was greatly reduced in the molecular layer of γ-2 PC-KO mice when compared to that of wild-type mice (**Figures 1C-1F**). To examine AMPA receptor-mediated responses of

PCs, we made whole-cell recordings from PCs in cerebellar slices and obtained instantaneous current-voltage relations during bath application of AMPA (2 μM) (Yamazaki et al., 2010) in the presence of cyclothiazide to minimize AMPA receptor desensitization. The average I-V relations were linear in both genotypes at P21, but the amplitude of membrane current was significantly lower in γ-2 PC-KO mice than in wild-type mice (**Figures 1G**). These results demonstrate that the expression of functional AMPA receptors in PCs is significantly reduced in γ-2 PC-KO mice.

We then compared AMPA-receptor mediated excitatory postsynaptic currents (EPSCs) of PCs between γ-2 PC-KO and wild-type mice. PCs receive two distinct glutamatergic inputs from climbing fibers (CFs) and parallel fibers (PFs), the axons of neurons in the inferior olive and granule cells in the cerebellar cortex, respectively (Ito, 1984; Palay and Chan-Palay, 1974). Previous studied show that EPSCs in PCs are mediated almost exclusively by AMPA receptors in the 2nd and 3rd postnatal weeks (Kakizawa et al., 2000; Kano et al., 1995; Llano et al., 1991). We stimulated CFs systematically in the granule cell layer beneath the PC under recording in cerebellar slices

from young adult mice at P21-43. In wild-type mice, large EPSCs were elicited in an all or none fashion in the majority of PCs, indicating that these PCs were innervated by single strong CFs (CF-mono) **(Figure 2A)**. In the rest of PCs, CF-EPSCs appeared with two or three distinct steps when the stimulus intensity was gradually increased or the stimulation site was systematically moved. Notably, each of the PCs with multiple CF steps had a single relatively large CF-EPSC and one or two relatively small CF-EPSCs, indicating that these PCs were innervated by single strong CFs (CF-multi-S) plus one or two weaker CFs (CF-multi-W) **(Figure 2A)** (Hashimoto et al., 2009; Hashimoto and Kano, 2003). In γ-2 PC-KO mice, the patterns of CF innervations of PCs were qualitatively similar to those of wild-type mice **(Figure 2A)**. However, the absolute amplitudes of EPSCs elicited by CF-mono, CF-multi-S and CF-multi-W were proportionally reduced to about 50 % of those of wild-type mice (CF-mono: Wild-type, 2227 ± 83.9 pA, n=70; γ-2 PC-KO, 1193 ± 70.4 pA, n=43; $p<0.0001$. CF-multi-S: Wild-type, 2314 ± 192.6 pA, n=27; γ-2 PC-KO, 1220 ± 74.1 pA, n=50; $p<0.0001$. CF-multi-W: Wild-type, 570 ± 94.1 pA, n=28; γ-2 PC-KO, 278 ± 35.1 pA, n=56; $p=0.0324$) (**Figures 2A and 2B**). These results indicate that

relative differences among EPSCs elicited by the three types of CF inputs are preserved, but their absolute synaptic strengths are proportionally reduced in γ-2 PC-KO mice at P21-P43. We then compared PF-mediated EPSCs between the two genotypes at P21-P49 by recording EPSCs during stepwise (1 μA) increase of PF stimulus strength. The input-output relations show that the PF-EPSC amplitude of γ-2 PC-KO mice was significantly reduced to about one third of that of wild-type mice (**Figure 2C and 2D**). Taken together, these data demonstrate that excitatory synaptic drive from the two types of inputs is globally reduced in PCs of γ-2 PC-KO mice.

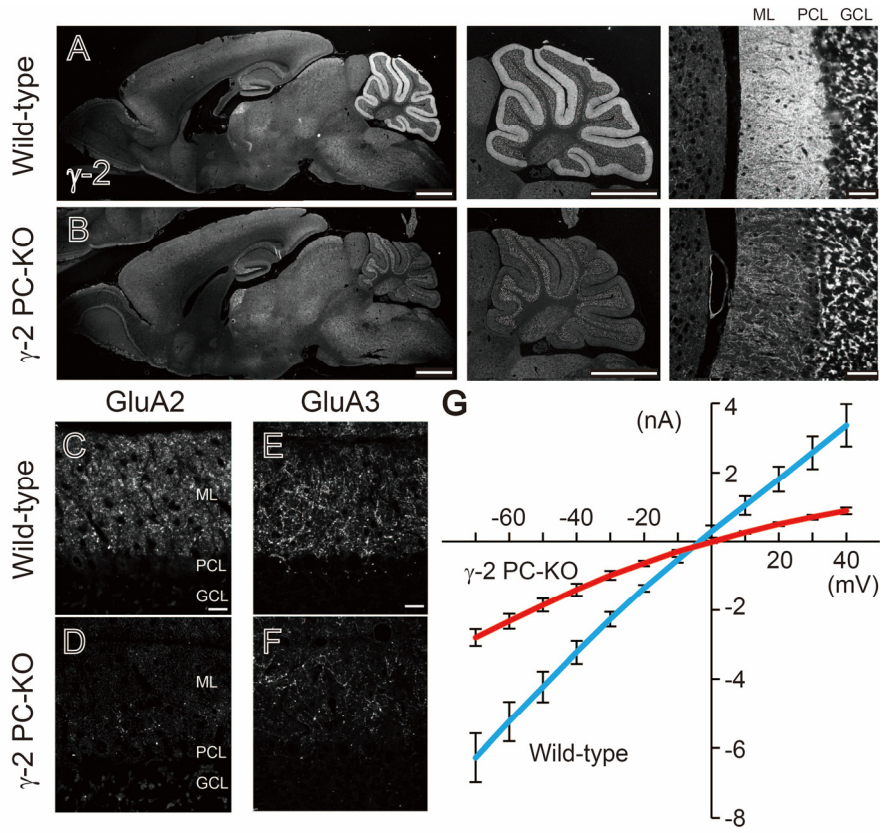

Figure 1. Generation of γ-2 PC-KO mice

(A & B) Immunohistochemistry for TARP γ-2 in the whole brain (Left), cerebellum (Middle) and cerebellar cortex (Right) in wild-type (A) and γ-2 PC-KO (B) mice at an adult age. ML: Molecular layer, PCL: Purkinje cell layer, GCL: Granule cell layer. In wild-type mice, γ-2 immunoreactivity is intense in the the ML and scattered in the GCL. In γ-2 PC-KO mice, γ-2 immunoreactivity in the ML is absent whereas that in the GCL is unchanged. Scale bars, 1 mm for (Left) and (Middle), 50 μm for (Right). (C -F) Immunohistochemistry for GluA2 (C, D) and GluA3 (E, F) in the cerebellar cortex in wild-type mice (C, E) and γ-2 PC-KO mice (D, F) at P21. Note a significant reduction of GluA2 (C, D) and GluA3 (E, F) immunoreactivity in the ML of γ-2 PC-KO mice. Scale bar, 20 μm. (G) I-V relationship of AMPA (2 μM)-induced currents in PCs of wild-type (n=5, blue line) and γ-2 PC-KO (n=4, red line) mice at P21. Membrane currents were measured during voltage ramp from +40mV to -70mV (duration 1.4sec). For leak subtraction, evoked currents in control external solusion were subtracted from those in

the presence of AMPA (2 μM). ACSF contained cyclothiazide (100 μM) and tetrodotoxin (0.5 μM). Liquid junction potential was corrected.

Error bars represent ±SEM.

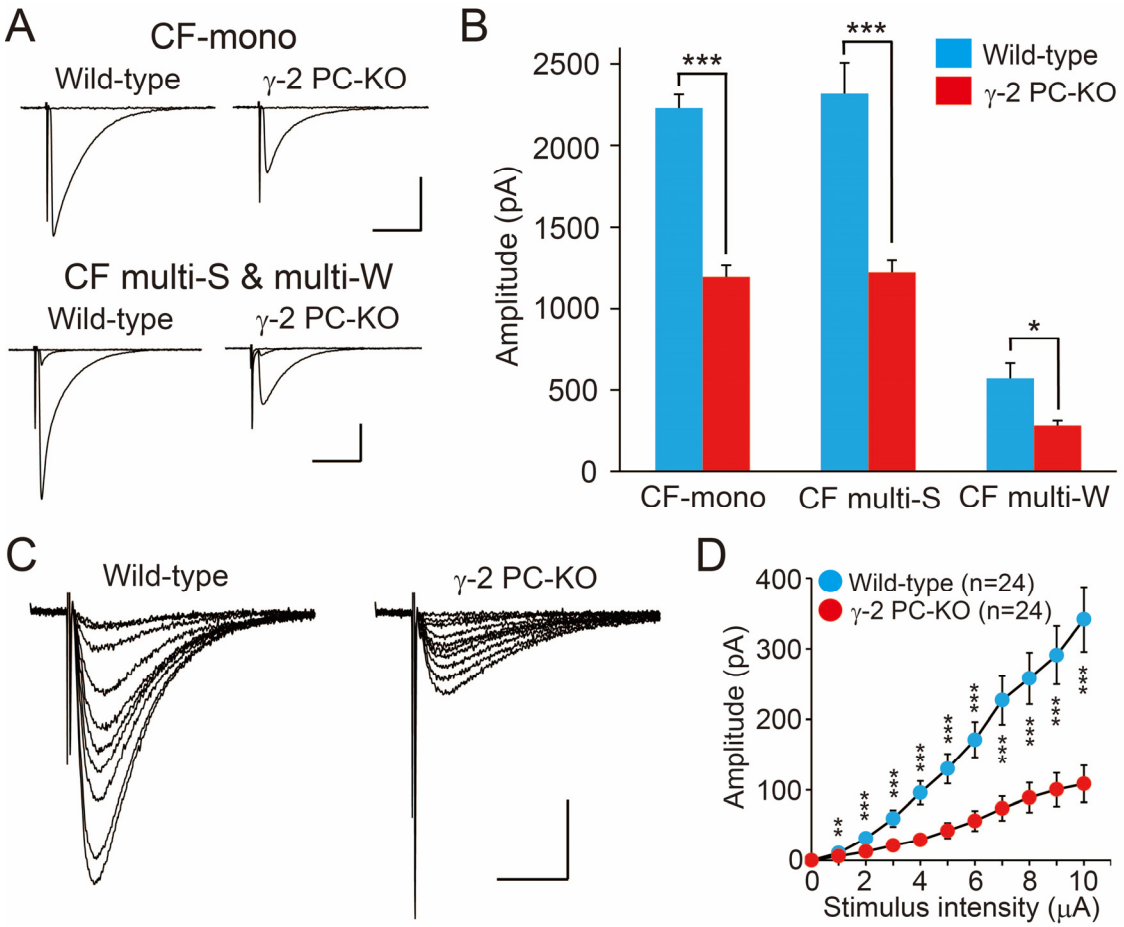

Figure 2. Strengths of excitatory synaptic inputs are decreased in γ-2 PC-KO mice

(A) Specimen records of EPSCs in PCs innervated by single CFs (CF-mono) (Upper) and in PCs multiply-innervated by strong (CF multi-S) and weak (CF multi-W) CFs from wild-type and γ-2 PC-KO mice (Lower) at P21-43. When stimulus intensity was changed, CF-EPSC appears in an all-or-none fashion. Two or three traces were superimposed at each threshold stimulus intensity. When a single step of CF-EPSC could be elicited, the CF was classified as "CF-mono." When multiple steps of CF-EPSCs were observed, the CF that elicited the largest CF-EPSC was classified as "CF multi-S" and the other CFs that elicited smallerr CF-EPSCs were classified as "CF multi-W." Scale bars, 10 ms and 1 nA. Holding potential, -20 mV. (B) Summary bar graphs showing the averaged peak amplitude of the three categories of CF-EPSC. Sample sizes of CF-EPSCs are 70 (CF-mono, wild-type), 43 (CF-mono, PC-KO), 27 (CF multi-S, wild-type), 50 (CF multi-S,

PC-KO), 28 (CF multi-W, wild-type) and 56 (CF multi-W, PC-KO). *:$p < 0.05$, ***:$p < 0.001$. (C) Specimen records of PF-EPSCs in wild-type and γ-2 PC-KO mice at P21-49. Stimulation of PFs with gradually increasing intensity elicits proportionally larger EPSCs. Ten traces recorded at different stimulus intensities (1 - 10 μA) were superimposed. Scale bars, 10 ms and 100 pA. Holding potential, -80 mV. (D) Input-output relationship of PF-EPSCs in wild-type and γ-2 PC-KO mice. Averaged peak amplitude at each stimulus intensity (1-10 μA) was plotted. **:$p < 0.01$, ***:$p < 0.001$.

Error bars represent ±SEM.

Reduced absolute synaptic strengths with normal disparity among multiple CF inputs to individual PCs in γ-2 PC-KO mice

Our previous studies show that relative difference between the strongest CF input and the other weaker CF inputs becomes progressively larger from P3 to P7 (Hashimoto and Kano, 2003). At the same time, the absolute values of total CF-EPSC amplitudes increased by about 4 folds (Hashimoto et al., 2011). Thus, we next examined developmental changes in the strength of CF synaptic inputs to PCs in wild-type and γ-2 PC-KO mice. First, to examine possible changes in the absolute synaptic strength, we measured the total amplitude of CF-EPSCs in each PC, which includes all of the recorded CF-EPSC steps. In wild-type mice the total CF-EPSC amplitude increased progressively from P3, reached a plateau at P9 and declined gradually after P12 (**Figures 3A and 3B**). CF-EPSCs in γ-2 PC-KO mice showed the same tendency of developmental change, but from P6 the total amplitude became significantly smaller than that of wild-type mice (**Figures 3A and 3B**). We examined expression of γ-2 protein in neonatal cerebellum and found that γ-2 was undetectable until P4 and its expression became obvious at P7 in the molecular layer and

the PC layer in wild-type mice (**Figures 4A-4F**). This developmental profile of γ-2 expression explains the result that the effect of γ-2 deletion on the absolute strength of CF-PC synapse first became obvious at P6 in γ-2 PC-KO mice (**Figures 3A and 3B**).

Second, in order to examine possible developmental changes in the relative difference of CF synaptic strengths, we calculated the disparity ratio that was used to quantify the relative difference among the strengths of multiple CFs innervating each PC (Hashimoto and Kano, 2003; Hashimoto et al., 2011). In wild-type mice the disparity ratio became progressively smaller from P3 and reached a plateau around P7 as reported previously (Hashimoto and Kano, 2003) (**Figure 3C**). In γ-2 PC-KO mice, the disparity ratio underwent a developmental change similar to that of wild-type mice (two-way ANOVA: $p=0.072$) (**Figure 3C**). We also calculated the fraction of the largest and the second largest CF-EPSC amplitudes relative to the total CF-EPSC amplitude from P3 to P9 (**Figure 3D**). There was no significant difference in the developmental changes of these values between the genotypes (two-way ANOVA: $p=0.122$) (**Figure 3D**). Moreover we recorded PF-EPSC at P12-16 and obtained the same result as in young adult age (data

not shown). Taken together, these results indicate that the absolute strengths of CF-PC and PF-PC synapses in PCs of γ-2 PC-KO mice become significantly smaller than those in wild-type mice at P6 and thereafter, whereas the relative differences in synaptic strengths among competing CF inputs are kept normal. Importantly, CF synapse elimination and CF translocation to PC dendrites occur in the same period (Watanabe and Kano, 2011). In the following sections, we investigated whether and how the reduced absolute synaptic strengths with normal disparity among multiple CF inputs to individual PCs affects CF synapse elimination and CF translocation.

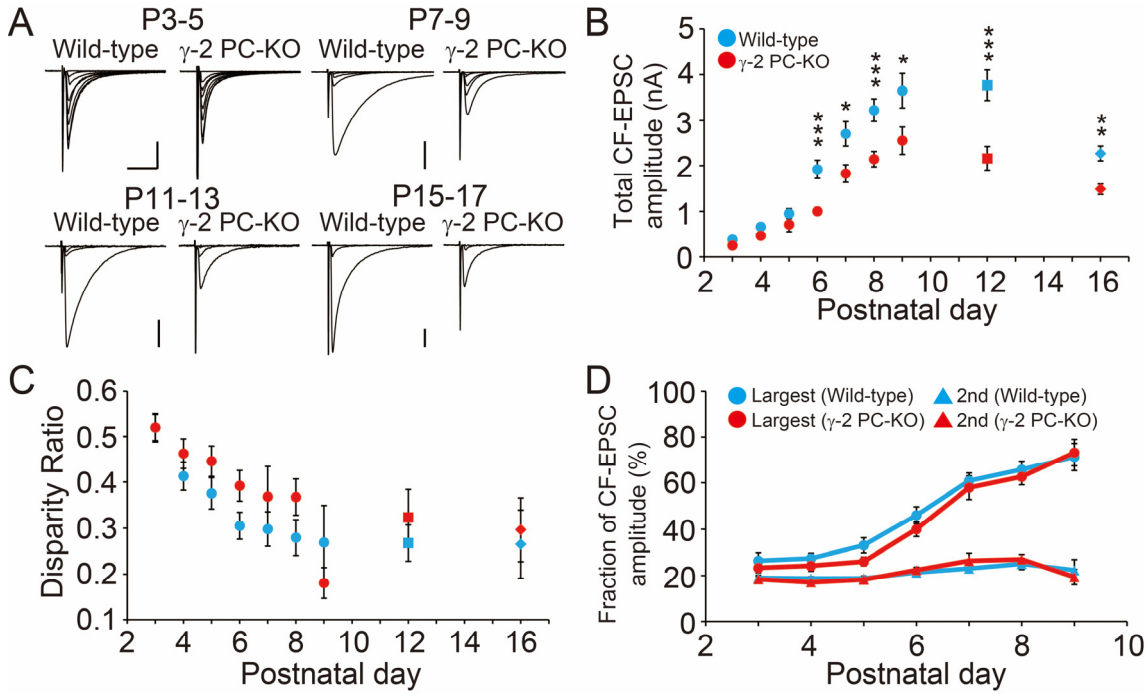

Figure 3. The absolute strengths of CF-PC synapses are decreased with normal relative difference in synaptic strengths among competing CFs in γ-2 PC-KO mice.

(A) Specimen records of CF-EPSCs at P3-5, P7-9, P11-13 and P15-17 in wild-type and γ-2 PC-KO mice. Scale bars, 10 ms and 500 pA. Holding potential, -80mV (P3-5) or -20mV (P7-9, P11-13 and P15-17). (B) Developmental changes in the total amplitude of CF-EPSCs recorded in each PC. The peak amplitudes of CF-EPSCs including all CF-EPSC steps were averaged at each age. Squares contain data from P11 to P13 and diamonds contain data from P15 to P17. The sample size for each genotype is 13-39 (wild-type mice) and 12-36 (γ-2 PC-KO mice). *:$p < 0.05$, **:$p < 0.01$, ***:$p < 0.001$. (C) Developmental changes in disparity ratio that was caluculated from PCs innervated by multiple CFs. The sample size for each genotype is 8-35 (wild-type mice) and 9-37 (γ-2 PC-KO mice). (D) Developmental changes in the fraction of CF-EPSC amplitude. To calculate the fraction of each step, the amplitude of individual CF-EPSC step was divided by total amplitude. The sample size for each genotype is 11-39 (wild-type mice) and 9-37 (γ-2 PC-KO mice).

Error bars represent ±SEM.

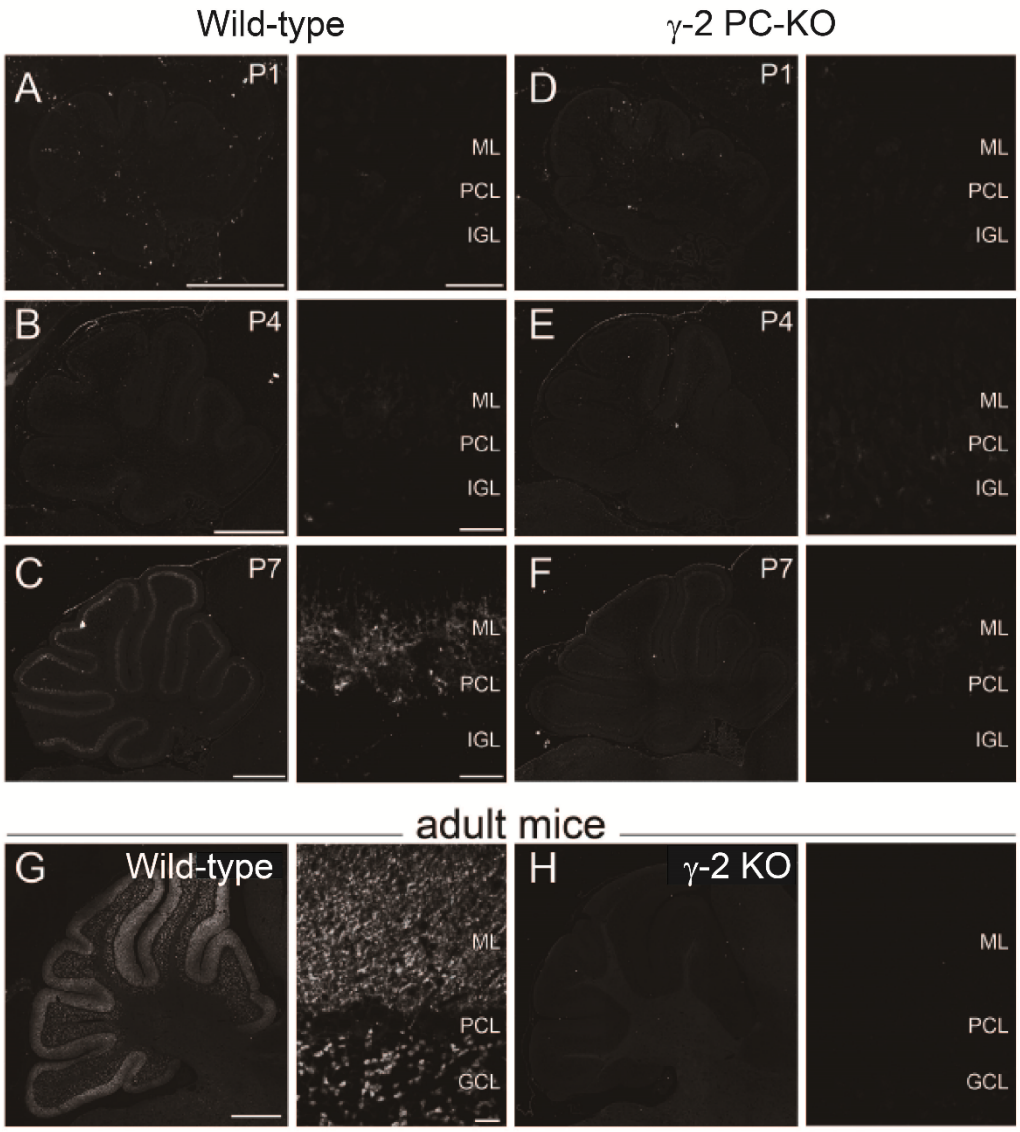

Figure 4. Expression of TARP γ-2 appears between P4 and P7.

(A-F) Immunohistochemistory for γ-2 in the cerebellum of wild-type and γ-2 PC-KO mice at P1, P4 and P7. In wild-type mice signals of γ-2 were hardly detectable at P4 and became obvious at P7. By contrast, the γ-2 signals were absent at P7 in γ-2 PC-KO mice. Scale bars, 500 μm (left) and 10 μm (right) for (A), 500 μm (left) and 20 μm (right) for B, C and G. (G, H) Confirmation of the specificity of the antibody against γ-2. Note that the signals for γ-2 immunofluorescence were absent in γ-2 global KO mice.

Impaired CF translocation and CF synapse elimination in γ-2 PC-KO mice

First we examined the extent of CF translocation by measuring the relative height of the most distal VGluT2 signals normalized by the thickness of the molecular layer at P21 (**Figure 5**)**.** While there was no change in the thickness of the ML (**Figure 5C**, Wild-type: 119 ± 2.7 μm; γ-2 PC-KO: 118.6 ± 2.3 μm; p=0.1440), the relative height of the tip of CF arbors was significantly lower in γ-2 PC-KO mice (**Figure 5D,** Wild-type: 69.6 ± 0.7 %; γ-2 PC-KO: 58.4 ± 0.5 %; p<0.0001). These results indicate that PC-specific deletion of γ-2 impairs dendritic translocation of strong CFs during postnatal cerebellar development.

We next tested whether CF synapse elimination was affected in γ-2 PC-KO mice. We estimated the number of CFs innervating each PC at P21-P43 from the number of distinct CF-EPSC steps in the same way as previous report (Mikuni et al., 2013; Nakayama et al., 2012). In wild-type mice, 73.7% (73/ 99) of PCs had single CF-EPSC steps and 26.3% (26/ 99) of PCs had two or more CF-EPSC steps (**Figures 6A and 6B**). In γ-2 PC-KO mice, less than half of PCs (46.5%, 60/126) had single CF-EPSC steps and. 53.5 % (66/126) of PCs had two or more CF-EPSC steps (**Figures 6A and 6B**). The

frequency distribution histogram of PCs in terms of the number of CF-EPSC steps shows significant difference between wild-type and γ-2 PC-KO mice ($p<0.0001$) (**Figure 6B**), indicating that CF synapse elimination is impaired in γ-2 PC-KO mice. To visualize CF innervations in the two genotypes, we injected a small amount of the anterograde tracer dextran Texas red (DTR) into the inferior olive and stained a subset of CFs. Then we performed triple fluorescent labeling experiments for calbindin (a PC marker), vesicular glutamate transporter type 2 (VGluT2, a CF terminal marker) and DTR (Miyazaki and Watanabe, 2011). In most PCs of wild-type mice, VGluT2 signals were not present on PC somata but were rich on proximal dendrites of PCs (**Figures 6C and 6D**), and essentially all the VGluT2 signal overlapped with DTR signals (**Figures 6C and 6D**). This result demonstrates that most of the wild-type PCs were innervated by single CFs on their proximal dendrites. In contrast, VGluT2 signals were frequently found on PC somata in γ-2 PC-KO mice (**Figures 6E-6H**). Moreover, PCs in γ-2 PC-KO mice were often associated with DTR/VGluT2-double positive CF terminals on proximal dendrites (**Figure 6F, 6H,** red arrows) and DTR-negative/VGluT2-positive CF terminals on the

soma (**Figure 6F, 6H,** green arrows). In some cases, DTR/VGluT2-double positive CF terminals (**Figure 6J,** red arrows) and DTR-negative/VGluT2-positive CF terminals (**Figure 6J,** green arrows) were co-localized on proximal dendrites of the same PCs (**Figure 6I, 6J**). These morphological data unequivocally demonstrate innervations of the PCs by multiple CFs. There was a significant difference between the genotypes in terms of the percentage of morphologically-determined mono and multiply-innervated PCs (**Figure 6K**). Taken together, these results indicate that PC-specific deletion of γ-2 impairs elimination of somatic CF terminals during postnatal cerebellar development.

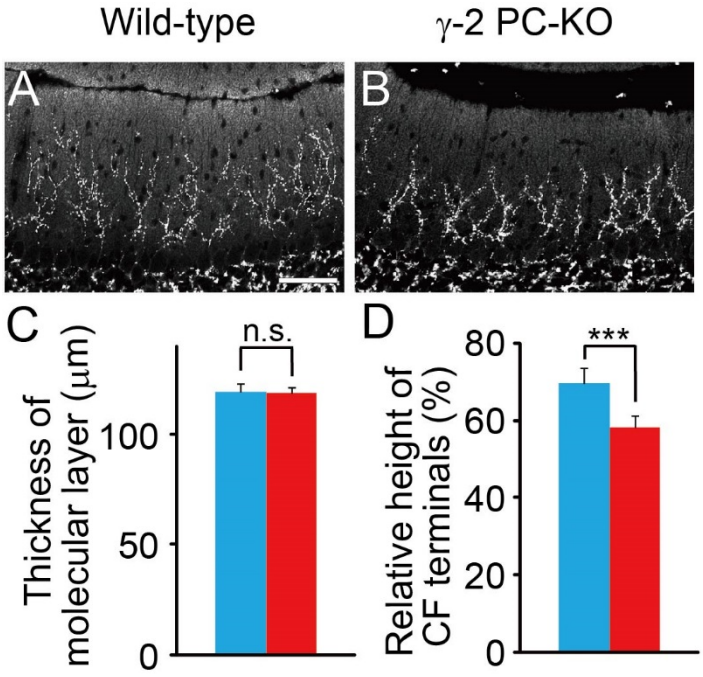

Figure 5. Relative height of CF terminals in the molecular layer is lower in γ-2 PC-KO mice than in Wild-type mice.

(A & B) Immunohistochemistry for VGluT2 in cerebellar cortex of Wild-type mice (A) and γ-2 PC-KO mice (B) at P21. Scale bars, 50 μm. (C) Summary bar graph of thickness of molecular layer in Wild type mice and γ-2 PC-KO mice. The vertical distance between pial surface and top of PC's soma was measured. (D) Summary bar graph of relative height of CF terminals in Wild type mice and γ-2 PC-KO mice. Length between highest VGluT2 signal and top of PC's soma was normalized by the thickness of molecular layer in each PC. ***: $p<0.001$.

Error bars represent ±SEM.

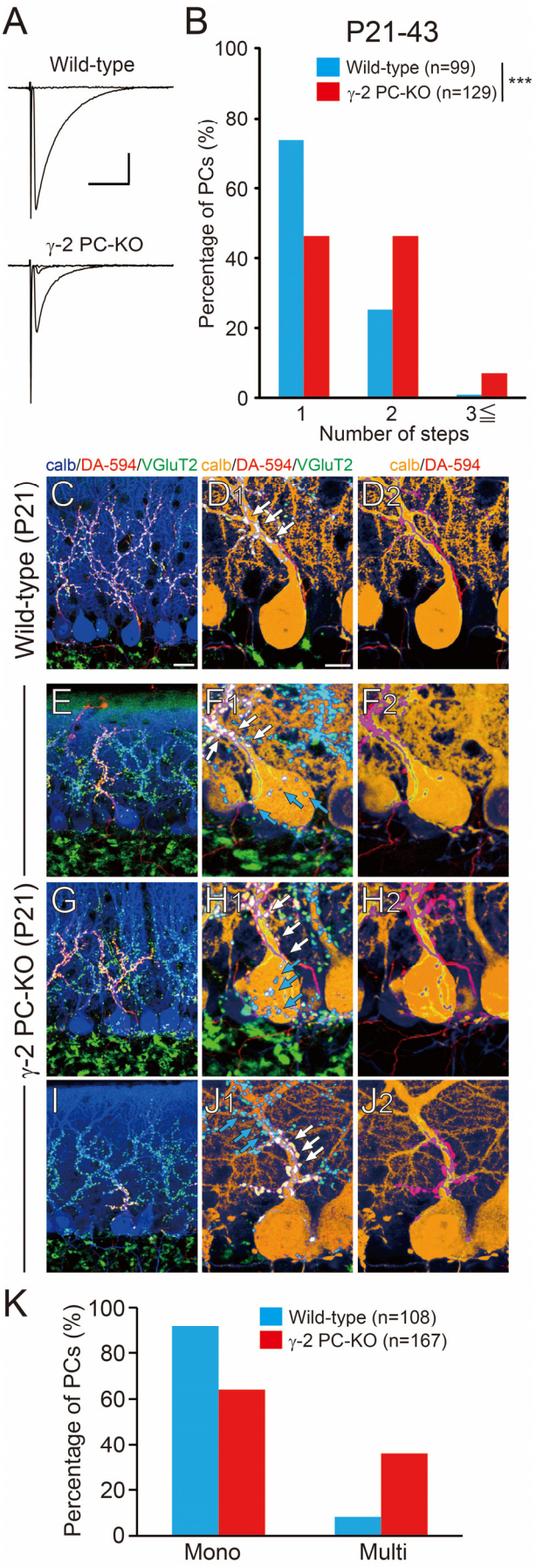
A
Wild-type
γ-2 PC-KO
B
P21-43
Wild-type (n=99)
γ-2 PC-KO (n=129)
***
Percentage of PCs (%)
100
80
60
40
20
0
1
2
3≦
Number of steps
calb/DA-594/VGluT2
calb/DA-594/VGluT2
calb/DA-594
Wild-type (P21)
γ-2 PC-KO (P21)
C
D1
D2
E
F1
F2
G
H1
H2
I
J1
J2
K
Wild-type (n=108)
γ-2 PC-KO (n=167)
Percentage of PCs (%)
100
80
60
40
20
0
Mono
Multi

Figure 6. CF synapse elimination is impaired in γ-2 PC-KO mice.

(A) Specimen records of CF-EPSCs in wild-type and γ-2 PC-KO mice. Scale bars, 10 ms and 500 pA. (B) Frequency distribution histgram for the number of CFs innervating each PC in wild-type and γ-2 PC-KO mice at P21-43. ***:$p<0.001$. (C-H) Triple immunostaining for calbindin (blue or ocher), anterogradely-labeled CFs (red, DA-594), and VGluT2 (green) in wild-type (C and D) and γ-2 PC-KO (E-J) mice at P21. D, F, H and J are the magnified views of C, E, G and I, respectively. Only PCs associated with anterograde tracer signals were analyzed. White and blue arrows in D1, F1, H1 and J1 indicate DTR-labeled/VGluT2-positive and DTR-unlabeled/VGluT2-positive CF terminals, respectively. Scale bars, 20 μm for (C, E, G, I) and 10 μm for (D, F, H, I). (K) Frequency distribution histgram of anatomically identified CF innervation pattern at P21. PCs were classified into those innervated by single CFs (mono) and by more than two CFs (Multi).

The late phase of CF synapse elimination is specifically impaired in γ-2 PC-KO mice

CF synapse elimination consists of two distinct phases, the early phase from P7 to around P11 and the late phase from around P12 to P17 (Watanabe and Kano, 2011). To clarify which phase is impaired in γ-2 PC-KO mice, we examined CF innervation patterns of PCs at P6-P8 (around the beginning of the early phase), P11-P13 (around the beginning of the late phase), and P15-17 (toward the end of the late phase). There was no significant difference between the genotypes in terms of the number of CF-EPSC steps either at P6-P8 ($p=0.4583$) (**Figure 7A**) or at P11-P13 ($p=0.705$) (**Figure 7B**). These results indicate that the early phase of CF elimination is normal in γ-2 PC-KO mice. In marked contrast, the frequency distributions show highly significant difference between the genotypes at P15-P17 ($p<0.0001$) (**Figure 7C**). While 80% of PCs were innervated by single CFs in wild-type mice, only 36.4% of PCs were innervated by single CFs and the rest of PCs were innervated by multiple CFs in γ-2 PC-KO mice (**Figure 7C**). These results demonstrate clearly that the late phase of CF elimination is specifically impaired in γ-2 PC-KO mice.

Previous studies have demonstrated that the metabotropic glutamate receptor subtype 1 (mGluR1) and its downstream signaling involving Gαq, phospholipase C β4 (PLCβ4), and protein kinase Cγ (PKCγ) is crucial for the late phase of CF elimination (Ichise et al., 2000; Kano et al., 1995; Kano et al., 1997; Kano et al., 1998; Offermanns et al., 1997). It is possible that the impaired CF synapse elimination in γ-2 PC-KO mice may result from reduced or altered mGluR1 signaling. To check this possibility, we first examined the expression of mGluR1 (**Figures 8A and 8B**), Gαq (**Figures 8C and 8D**), PKCγ (**Figures 8E and 8F**) and PLCβ4 (**Figures 8G and 8H**) by immunohistochemistry. We found that these molecules are normally expressed in PCs of γ-2 PC-KO mice. Then we tested whether mGluR1 signaling is functional in PCs of γ-2 PC-KO mice. Repetitive PF stimulation has been shown to induce slow EPSCs in PCs that are mediated by mGluR1, Gαq, PLCβ4 and TRPC3 channel (Hartmann et al., 2008; Mitsumura et al., 2011). In the presence of the AMPA receptor blocker NBQX (10 μM), brief high-frequency trains of PF stimulation (5 pulses of PF stimulation at 100Hz, 100μA) readily induced slow EPSCs in PCs of γ-2 PC-KO mice whose peak amplitude were in the same

range as those in PCs of wild-type mice (Wild-type: 651.7 ± 113.5 pA; γ-2 PC-KO: 583.3 ± 106.7 pA; p=0.9719) (**Figures 8I and 8J**). The slow EPSCs were abolished by adding an mGluR1 antagonist, CPCCOEt (100 μM) to the bathing solution (**Figure 8I**). These results clearly indicate that the mGluR1 signaling is normal in PCs of γ-2 PC-KO mice.

GABAergic inhibition to PC somata from molecular layer interneurons is also important for the regulation of the late phase CF elimination (Nakayama et al., 2012). We checked whether the morphology and function of molecular layer interneurons were altered in PCs of γ-2 PC-KO mice. We made double immunofluorescence staining for calbindin, a PC marker, and palvalbmin (PA), a marker for MLI and PC, or single immunostaining for VGAT, a marker of GABAergic presynapse, and found that there was no difference between wild-type and γ-2 PC-KO mice. (**Figures 9A-9D**). Furthermore, we recorded mIPSCs from PCs at P12-P16 and found that there was no difference between the two mouse strains in the frequency (Wild-type: 3.8 ± 0.9 Hz; γ-2 PC-KO: 4.0 ± 0.9 Hz; p=0.9728) or the amplitude (Wild-type: 73.4 ± 10.2 pA; γ-2 PC-KO: 54.1±4.4 pA; p=0.1423) (**Figures 9E-9G**). These results indicate that GABAergic

inhibition to PC somata from molecular layer interneurons is normal in γ-2 PC-KO mice. Taken together, the impaired CF synapse elimination in γ-2 PC-KO mice is considered to be caused by mechanisms other than the impairment of mGluR1 signaling in PCs or the attenuation of GABAergic inhibition to PC somata.

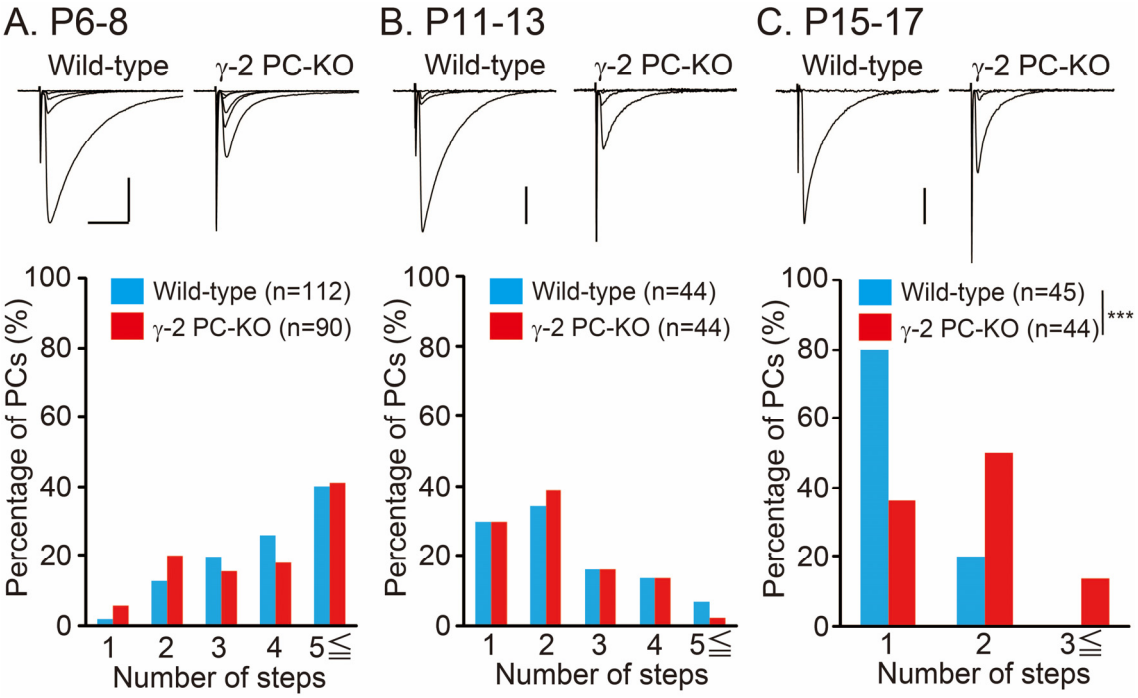

Figure 7. The late phase of CF synapse elimination is impaired in γ-2 PC-KO mice.

Specimen records of CF-EPSCs (upper poanels) and frequency distribution histgrams for the number of CFs innervating each PC (lower panels) in wild-type and γ-2 PC-KO mice at P6-8 (A), P11-13 (B) and P15-17 (C). Scale bars, 10 ms and 500 pA. ***:p<0.001.

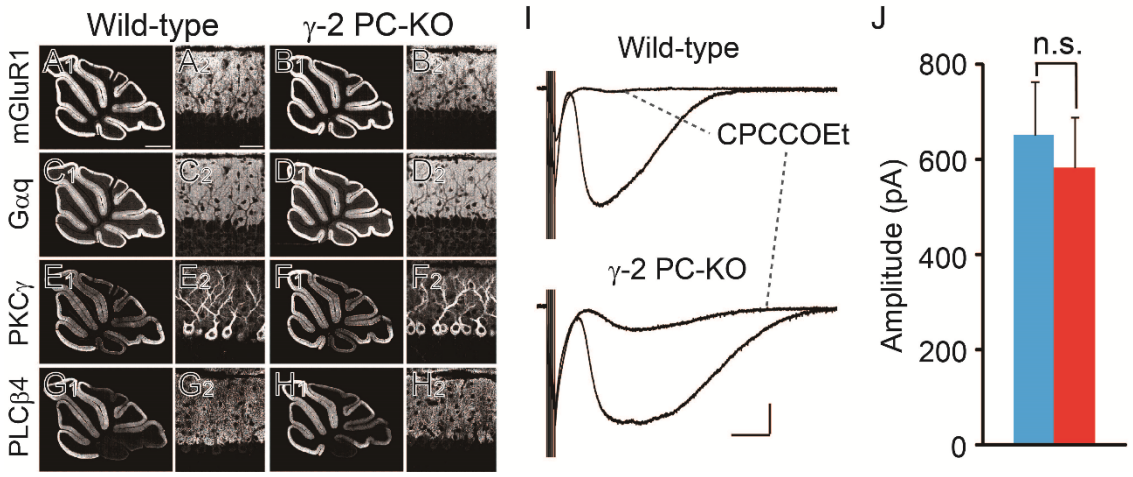

Figure 8. Unaltered mGluR1 signaling in γ-2 PC-KO mice.

(A-H) Immunohistochemistry for mGluR1 (A, B), Gαq (C, D), PKCγ (E, F) and PLCβ4 (G, H) in the cerebellum of wild-type and γ-2 PC-KO mice. Scale bars, 500 μm for (A1-H1) and 50 μm for (A2-H2). (I) Specimen records of mGluR1-mediated slow EPSC in wild-type (upper) and γ-2 PC-KO (lower) mice. A tungsten electrode was placed on the outer half of molecular layer and a train of 5 stimuli (100 Hz, 100 μA) was applied. Slow EPSCs were mostly blocked by an mGluR1 blocker, CPCCOEt (100 μM). Scale bars, 200 ms and 200 pA. (J) Summary bar graph showing averaged peak amplitudes of mGluR1-mediated slow EPSCs in wild-type (n=10) and γ-2 PC-KO (n=11) mice. There was no significant difference between the two genotypes.

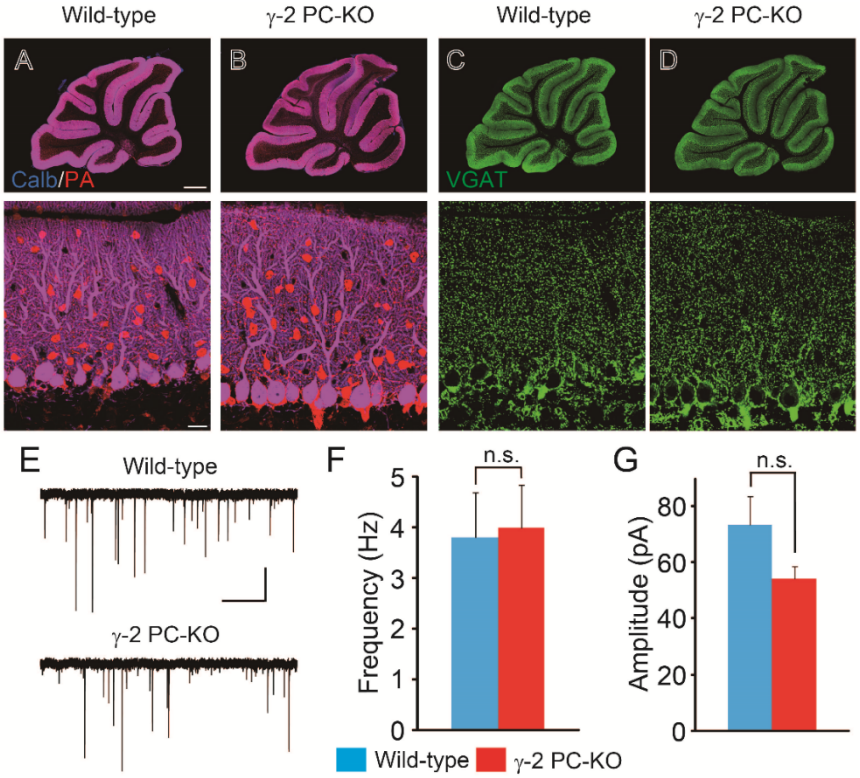

Figure 9. GABAergic inhibition to PCs is unaltered in γ-2 PC-KO mice.

(A, B) Double immunostaining of the cerebellar cortex for calbindin, a PC marker, and palvalbmin (PA), a marker of molecular layer interneurons (MLIs) in wild-type (A) and γ-2 PC-KO (B) mice. Lower panels represent magnified views of respective upper panels. Note apparently normal distribution of PV (+) MLIs in γ-2 PC-KO mice. Scale bars, 500 μm (upper) and 20 μm (lower). (C, D) Immunostaining of the cerebellar cortex for VGAT, a marker of GABAergic presynaptic terminals in wild-type (C) and γ-2 PC-KO (D) mice. Note apparently normal pattern of VGAT immunostaining in γ-2 PC-KO mice. (E) Specimen records of mIPSCs from PCs of wild-type (upper) and γ-2 PC-KO (lower) mice. mIPSCs were recorded in the presence of NBQX (10 μM), R-CPP (5 μM) and tetrodotoxin (0.5 μM). Scale bars, 1s and 100 pA. Holding potential, -20 mV. (F, G) Summary bar graphs showing average mIPSC frequencies (F) and amplitudes (G) at P12 to P16 in wild-type (n=8) and γ-2 PC-KO (n=14) mice.

Error bars represent ± SEM.

CF-mediated Ca^{2+} influx through P/Q-type VDCC is attenuated in γ-2 PC-KO mice

We have reported recently that the late phase of CF elimination is dependent on the immediate early gene *Arc* that is activated by Ca^{2+} influx to PCs through P/Q-type VDCC (Mikuni et al., 2013). Since the amplitude of CF-EPSCs in γ-2 PC-KO mice is reduced to about half that in wild-type mice, it is possible that CF-induced Ca^{2+} transients through activation of P/Q-type VDCC are significantly reduced in PCs of γ-2 PC-KO mice. The reduction of Ca^{2+} influx may in turn result in insufficient activation of *Arc* and impairment of CF synapse elimination. To test this hypothesis, we first examined whether the function of P/Q-type VDCC was altered in PCs of γ-2 PC-KO mice at P12-16 when the late phase of CF synapse elimination proceeds. We made whole-cell recordings from PC somata, filled entire PCs with a Ca^{2+} indicator dye, Oregon Green 488 BAPTA-1 (OGB-1), and depolarized PCs from -80mV to -10mV for 1 s under the voltage-clamp mode (Mikuni et al., 2013; Nakayama et al., 2012). Both wild-type mice and γ-2 PC-KO mice showed large increases of fluorescent calcium signals (**Figure 10A)** and there was no significant difference in the integral for 3 s from the initial rise between the two mouse strains (Wild-

type: 560 ± 140 % * s; γ-2 PC-KO: 385 ± 57.4 % * s; p=0.7508) **(Figure 10B)**. The depolarization-induced calcium signals were reduced by about 60% in the presence of a specific P/Q-type VDCC blocker, ω-agatoxin IVA (0.4 μM) (Wild-type: 57.9 ± 7.2 %; γ-2 PC-KO: 63.9 ± 7.2 %; p=0.7508) (**Figures 10B and 10C**). These results indicate that P/Q-type VDCC functions normally in PCs of γ-2 PC-KO mice. We next examined whether CF-induced calcium transients were altered in γ-2 PC-KO mice at P12-16. Under current-clamp mode, stimulation of the strongest CF in the recorded PC induced typical complex spikes in both wild-type and γ-2 PC-KO mice (**Figures 10D)**. However, the resultant calcium transients in γ-2 PC-KO mice were significantly smaller than those in wild-type mice (**Figures 10E**).The peak amplitude of Ca^{2+} transient in γ-2 PC-KO mice was about half of that in wild-type mice (wild-type: 24.5 ± 3.4 %; γ-2 PC-KO: 11.9 ± 3.2 %; p=0.0074) (**Figure 10F**). These results clearly indicate that CF-induced Ca^{2+} transients are significantly reduced in PCs of γ-2 PC-KO mice because of the smaller CF-EPSP amplitude and reduced activation of P/Q-type VDCC at the late phase of CF synapse elimination.

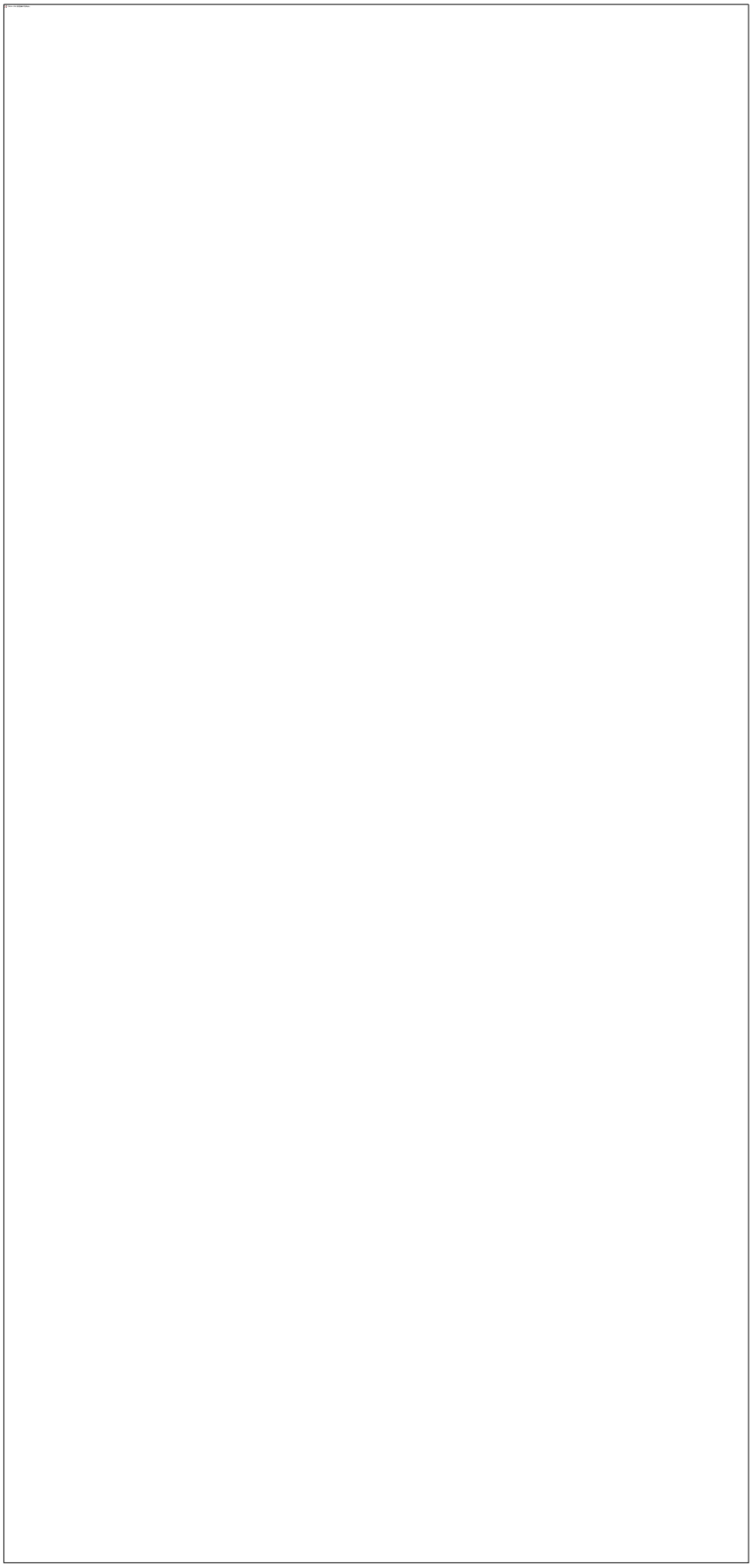

Figure 10. CF-induced Ca^{2+} transients in PCs through P/Q-type voltage-gated Ca^{2+} channels are attenuated in γ-2 PC-KO mice at P12-16.

(A) Representative images showing depolarization-induced changes in the fluorescence intensity of OGB-1 in wild-type (Upper) and γ-2 PC-KO (Lower) PCs. A Ca^{2+} indicator, OGB-1 (100 μM) was infused into PCs through a recording pippete. ω-Aga (+) indicates the data in the presence of a P/Q-type VDCC blocker, ω-Agatoxin IVA (0.4 μM). Regions of interest (ROIs) are surrounded by red dots. Scale bar, 20 μm. (B) Representative traces showing depolarization-induced changes in the OGB-1 fluorescence in wild-type and γ-2 PC-KO PCs. Black traces indicate the fluorescence change recorded in ω-Agatoxin containing ACSF. Green dot bars show the integrated period for (C). Scale bars, 4 s and 50 %. (C) Summary bar graph showing the fraction of ω-Agatoxin-sensitive component in wild-type (n=9) and γ-2 PC-KO mice (n=7). (D) Representative images showing changes in the OGB-1 fluorescence intensity induced by evoked CF-inputs in wild-type (upper panels) and γ-2 PC-KO (lower panels) mice. ROIs are surrounded by red dots. Scale bar, 20 μm. Voltage traces on the right are complex spikes recorded simultaneously with Ca^{2+} transients from the same PCs. Scale bars, 20 ms and 20 mV. (E) Representative traces showing normalized changes in the OGB-1 fluorescence intensity by CF inputs in wild-type and γ-2 PC-KO mice. Scale bars, 1s and 5 %. (F) Summary bar graph showing the average peak amplitudes of CF-induced Ca^{2+} transients in wild-type (n=11) and γ-2 PC-KO mice (n=12). **:$p < 0.01$.

Error bars represent ± SEM.

Rescue of the impaired CF synapse elimination by overexpression of Arc in PCs of γ-2 PC-KO mice

The reduced Ca^{2+} transients by CF inputs is considered to result in insufficient activation of *Arc*, which may leads to the impairment of the late phase of CF elimination. However, it is difficult to detect differences in *Arc* expression between the two genotypes, because its basal expression level is extremely low. We took consequently an alternative approach to test the aforementioned possibility. If insufficient *Arc* activation is a cause of the impaired CF synapse elimination in γ-2 PC-KO mice, PC-specific overexpression of *Arc* by lentivirus vectors (Torashima et al., 2006; Uesaka et al., 2012) should rescue the phenotype. We injected lentiviruses carrying the *GFP* and *Arc* sequences to the cerebellum of γ-2 PC-KO mice at P3-P5 (**Figure 11**). After the mice grew up to P19-P23, acute cerebellar slices were prepared and whole-cell recordings were performed from GFP-positive PCs with *Arc* overexpression (Arc-OE) and GFP-negative uninfected control PCs in the same slices (Mikuni et al., 2013). In control PCs, less than half of the PCs (45.1%) were innervated by single CFs and the rest were innervated by multiple CFs,

which is consistent with the data from untransfected γ-2 PC-KO mice (**Figure 6**). In contrast, 67.3% of the PCs were mono innervated and the rest were multiply-innervated in PCs with Arc OE (**Figures 12A and 12B**). The frequency distribution was significantly different between control and Arc OE PCs ($p=0.027$), while there was no significant difference in the frequency distribution between control and PCs with GFP expression alone (**Figures 11C and 11D**). These results indicate that Arc overexpression in PCs effectively rescued the impaired CF synapse elimination of γ-2 PC-KO mice.

To further confirm that Arc-dependent CF synapse elimination is impaired in γ-2 PC-KO mice, we tested the effect of PC-specific Arc knockdown. Previous report showed that Arc knockdown in wild-type mice impairs CF synapse elimination in the late phase (Mikuni et al., 2013). However, if in γ-2 PC-KO mice Arc-mediated CF synapse elimination is occluded, Arc knockdown in γ-2 PC-KO mice must not show an additive effect in the impaired synapse elimination. In the same way as previous report (Mikuni et al., 2013), Lentivirus vectors carrying the *GFP* sequence and micro RNA against *Arc* were injected into the cerebellum of γ-2 PC-KO mice at P1-P3 (**Figure 11**), and CF

innervation patterns were examined in acute cerebellar slices at P19-P23. As shown in Figure 8C and 8D, there was no significant difference in CF innervations patterns between uninfected control and Arc knockdown PCs in the same slices (p=0.499) (**Figure 12C & 12D**), indicating that Arc knockdown had no additive effect on CF innervations in γ-2 PC-KO mice. Taken together, these results demonstrate that the failure to activate Arc presumably because of the reduced CF-induced Ca^{2+} transients is a major cause of the impairment of the late phase of CF elimination in γ-2 PC-KO mice.

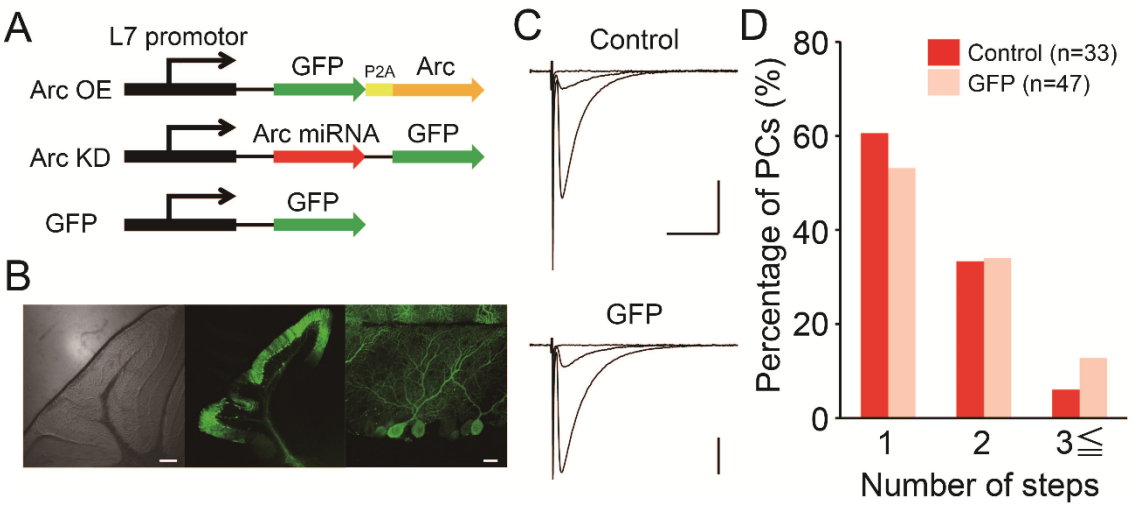

Figure 11. GFP expression alone does not promote CF synapse elimination in γ-2 PC-KO mice.

(A) Scheme of constructs for Arc overexpression (Arc OE), Arc knockdown (Arc KD) and GFP expression alone (GFP). (B) Representative images of cerebellar slices from a virus-injected mouse at P20-24. An injection needle was placed on the surface of the cerebellar vermis. Infected PCs were identified with GFP signals. Scale bars, 200 μm for (left and middle), 20 μm for (right). (C) Specimen records of CF-EPSCs in GFP-negative control PCs and GFP-expressing PCs. Scale bars, 10 ms and 500 pA. (D) Frequency distribution histogram for the number of CFs innervating each PC in control and GFP-expressing PCs.

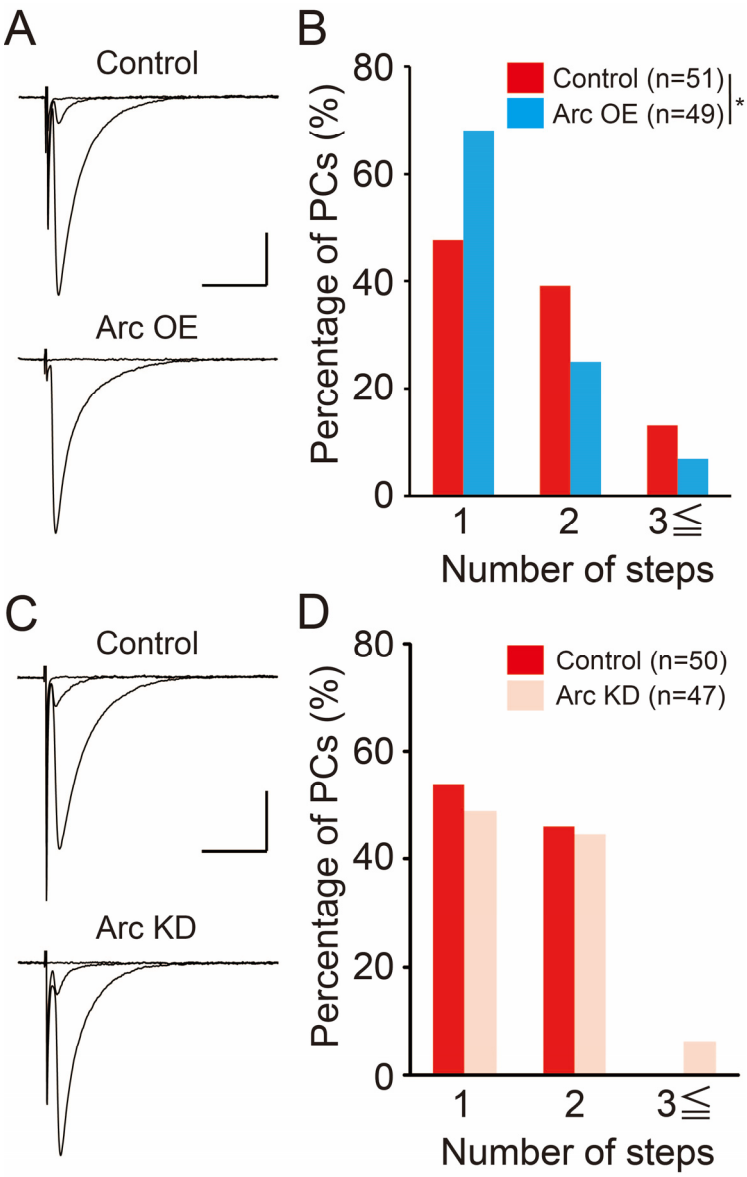

Figure 12. CF synapse elimination mediated by Arc is impaired in γ-2 PC-KO mice. (A) Specimen records of CF-EPSCs in GFP-negative control PCs and GFP-expressing PCs with Arc overexpression (OE). At P3-5, viruses carrying GFP and Arc were injected to the cerebellar vermis. Infected PCs were identified by GFP signals. At P19-23, the number of CFs innervating each PC was examined. Scale bars, 10 ms and 500 pA. *:$p < 0.05$. (B) Frequency distribution histgrams for the number of CFs innervating each PC in GFP-negative control PCs and GFP-expressing PCs with Arc OE. (C) Specimen records of CF-EPSCs in GFP-negative control PCs and GFP-expressing PCs with Arc knockdown (KD). At P1-2 viruses carrying GFP and Arc miRNA were injected to the

cerebellar vermis. At P19-25 the number of CFs innervating each PC was examined. Scale bars, 10 ms and 500 pA. (D) Frequency distribution histgrams for the number of CFs innervating each PC in GFP-negative control PCs and GFP-expressing Arc KD PCs.

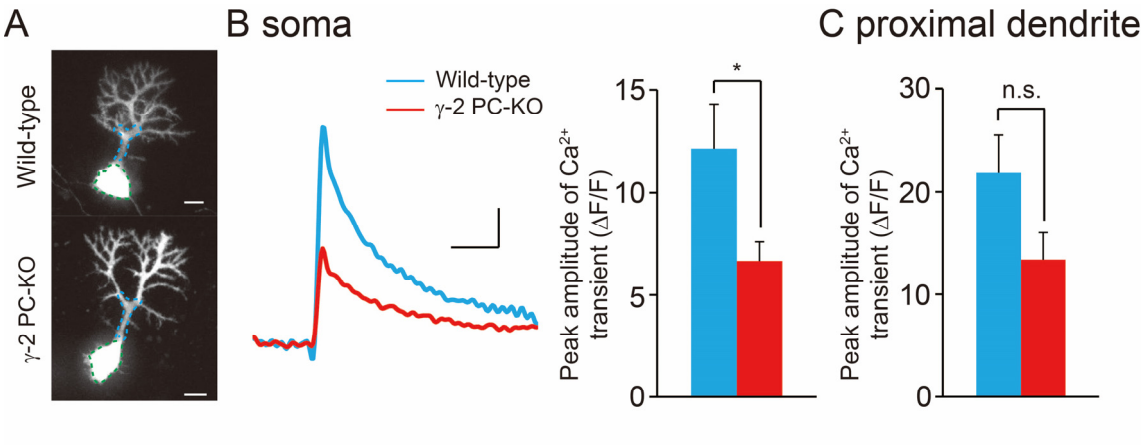

Figure 13. CF-induced Ca^{2+} transients in PC somata are attenuated in γ-2 PC-KO mice at P7-9

(A) Representative images of PCs filled with OGB-1 in wild-type (upper) and γ-2 PC-KO (lower) PCs. Regions of interest (ROIs) are surrounded by green (somata) and blue (proximal dendrite) dots. Scale bar, 10 μm. (B) (left) Averaged traces showing normalized changes in the OGB-1 fluorescence intensity by CF inputs in PC somata of wild-type and γ-2 PC-KO mice. Scale bars, 1s and 2 %. (right) Summary bar graph showing average peak amplitudes of CF-induced Ca^{2+} transients in PC somata of wild-type (n=11) and γ-2 PC-KO mice (n=11). *:$p< 0.05$. (C) Summary bar graph showing average peak amplitudes of CF-induced Ca^{2+} transients in proximal dendrite of wild-type (n=10) and γ-2 PC-KO mice (n=11). Error bars represent ± SEM.

DISCUSSION

We addressed the question whether global scaling down of excitatory synaptic inputs to whole neurons without changing relative difference in synaptic strength between excitatory inputs affects refinement of excitatory synaptic organization during postnatal developmental. We examined CF to PC synapse elimination in developing cerebellum as a model of synapse refinement, and generated γ-2 PC-KO mice to globally scale down excitatory synaptic inputs to whole PCs. The development of CF-PC synapses up to P5 was normal in γ-2 PC-KO mice (**Figure 3**), because the expression of γ-2 was undetectable at P4 (**Figure 4**) and the contribution of γ-2 is thought to be negligible for CF synapse development during the first 5 postnatal days. Consequently, the selective strengthening of single CF inputs in individual PCs, which occurs during the first postnatal week (Hashimoto and Kano, 2003), was normal in γ-2 PC-KO mice (**Figure 3**). In contrast, from P6 and thereafter, the absolute amplitudes of EPSCs from both strong and weak CFs in γ-2 PC-KO mice were reduced proportionally to about half of that of wild-type mice (**Figure 3**). Thus, γ-2 PC-KO mice after P6 can be used as an ideal model

in which absolute synaptic strengths were scaled down while preserving relative difference in synaptic strengths between excitatory inputs. We examined the three aspects of CF synapse elimination, which occur after P7, in γ-2 PC-KO mice.

Impaired dendritic CF translocation in γ-2 PC-KO mice

We have shown previously that P/Q-type VDCC is indispensable for the dendritic CF translocation from P9 (Hashimoto et al., 2011). In γ-2 PC-KO mice, the height of CF arbors relative to the thickness of the molecular layer was lower, whereas the molecular layer thickness was similar when compared to the wild-type mice (**Figure 5**), indicating a moderate impairment of dendritic CF translocation. This presumably results from the reduced Ca^{2+} transients in PC dendrites in response to CF synaptic inputs in γ-2 PC-KO mice. We have reported previously that the extension of CF arbors are impaired in myosin Va mutant mice and rats (Takagishi et al., 2007) in which dendritic spines of PCs are devoid of smooth endoplasmic reticulum and therefore the amplitude of inositol tris-phosphate-induced Ca^{2+} release in PC dendritic spines were reduced (Miyata et al., 2000).

Moreover, the amplitude of CF-EPSCs was significantly reduced in the myosin Va mutant mice (Takagishi et al., 2007), which would lead to reduction in CF-induced Ca^{2+} transients in PC dendrites. These results strongly suggest that reduced Ca^{2+} signaling in PC dendrites from P9 results in impairment of dendritic translocation of CFs.

The early phase of CF synapse elimination is not affected in γ-2 PC-KO mice

We have reported previously that PC-selective deletion of P/Q-type VDCC impairs CF functional differentiation and the early phase of CF synapse elimination (Hashimoto et al., 2011). Based on these results, it has been thought that sufficient Ca^{2+} influx into PCs through P/Q-type VDCC was required for the early phase of CF synapse elimination. In γ-2 PC-KO mice, CF-induced somatic Ca^{2+} transients were significantly smaller also at P7-9 when the early phase of CF synapse elimination proceeds (**Figure 13**). However the early phase of CF synapse elimination was not impaired in γ-2 PC-KO (**Figure 7**). Then what is the most important factor in the early phase of CF synapse elimination? During this developmental period, PC dendrites are still immature and CF synapses are mostly

on PC somata. Although a single winner CF begins dendritic translocation at P9 in each PC, synapses of the winner CF and those of the other loser CFs are located spatially near on the soma (Hashimoto et al., 2009). A recent *in vivo* time-lapse imaging of CF elimination has shown that CF terminals are highly motile on the soma, but their motility is significantly reduced on dendrites (Carrillo et al., 2013). Therefore the translocating CF will become the winner, while the CFs remaining on the soma will be the losers and will be eliminated. Interestingly photo-ablation of the winner CF induced the translocation of an alternative CF which otherwise would have become a loser CF. These results suggest that multiple CFs compete for limited resources with one another to become a winner in each PC. It is therefore likely that the relative difference in synaptic strengths among competing CF inputs is an important factor to determine a single winner CF in each PC

Impairment of the late phase of CF synapse elimination due to insufficient Arc activation in γ-2 PC-KO mice

We found that the late phase of CF synapse elimination was impaired in γ-2 PC-KO mice (**Figure 7**). The mGluR1 to protein kinase Cγ (PKCγ) signaling pathway in PCs and GABAergic inhibition to PC somata from molecular layer interneurons have been shown to be essential for the late phase of CF synapse elimination (Ichise et al., 2000; Kano et al., 1995; Kano et al., 1997; Kano et al., 1998; Nakayama et al., 2012; Offermanns et al., 1997). Our results, however, indicate that both mGluR1 signaling and GABAergic inhibition are normal in PCs of γ-2 PC-KO mice (**Figures 8 and 9**). In contrast, while the function of P/Q-type VDCC was normal, CF-induced Ca^{2+} transients due to activation of P/Q-type VDCC in PC's proximal dendrites were significantly reduced in γ-2 PC-KO mice (**Figure 10**). Since Arc mediates the late phase of CF synapse elimination downstream P/Q-type VDCC (Mikuni et al., 2013), we investigated the possibility of insufficient Arc activation in γ-2 PC-KO mice. Lentivirus-mediated overexpression of Arc into PCs of γ-2 PC-KO mice could rescue their impairment of the late phase of CF

synapse elimination (**Figure 12A**). On the other hand, knockdown of Arc in PCs of γ-2 PC-KO mice had no additive effect regarding the late phase of CF synapse elimination (**Figure 12B**). From these results, we conclude that the Arc-dependent CF synapse elimination is impaired in γ-2 PC-KO mice due to reduced CF-induced Ca^{2+} signaling in PC dendrites and insufficient activation of Arc.

We have recently reported that Arc activation is necessary but is not sufficient by itself for the late phase of CF synapse elimination (Mikuni et al., 2013). This notion is based on the observation that Arc overexpression did not rescue the impairment of CF synapse elimination by knockdown of P/Q-type VDCC. We therefore assume that Arc may cooperate with other factors induced by P/Q-type VDCC-mediated Ca^{2+} elevation in PCs to accomplish the late phase of CF synapse elimination. In the present study, we demonstrate that Arc overexpression alone effectively rescued the impairment of the late phase of CF synapse elimination. This is presumably because Arc could not be sufficiently activated but the factors that cooperate with Arc would be activated sufficiently in PCs of γ-2 PC-KO mice. Arc overexpression alone may fulfill the

requirements for the elimination of redundant CF synapses from the soma. Arc has been reported to play important roles in LTD in hippocampus neurons (Plath et al., 2006) and cultured PCs (Smith-Hicks et al., 2010). One possibility is that activated Arc in PCs may contribute to the induction of LTD at CF-PC synapses (Hansel and Linden, 2000) and may facilitate the removal of CF synapses from PC somata (Mikuni et al., 2013).

The present results suggest that the absolute strengths of CF synaptic inputs and the intracellular Ca^{2+} levels in PCs are crucial for the late phase of CF synapse elimination. Using *in vivo* time-lapse imaging of the behavior of living CFs, Carrillo et al. has recently reported that only one CF can translocate to the dendrites whereas their competitors are restricted to perisomatic regions, and that the CF that begins dendritic translocation becomes the winner and monopolizes PC dendrites (Carrillo et al., 2013). During the period of the late phase CF synapse elimination, single winner CFs widely innervate PC dendrites whereas synapses of the other loser CFs are confined to PC somata in individual PCs (Hashimoto et al., 2009). Since EPSCs of the strongest CF are on average about 4 times larger than those of the other CFs (Hashimoto and Kano, 2003), it is highly unlikely

that a weaker CF overcomes the predominant CF and eventually becomes the winner. These results support the notion that CF monoinnervation of dendrites of each PC is established by non-selective elimination of perisomatic synapses originating from both the winner and the other CFs during the late phase of CF synapse elimination (Hashimoto et al., 2009). The major role of the winner CF would be to induce Ca^{2+} transients in dendrites which are large enough to activate Arc that facilitates elimination of perisomatic CF synapses. It is therefore reasonable that absolute CF synaptic strengths are a crucial factor for the late phase of CF synapse elimination.

In conclusion, relative differences in synaptic strengths are important during developmental period when multiple synaptic inputs are competing for postsynaptic sites, such as the phase of functional differentiation and the early phase of CF synapse elimination. In contrast, absolute synaptic strengths have important meanings at developmental stage in which the winner and loser synaptic inputs have been determined, such as the late phase of CF synapse elimination. Thus, neurons appear to utilize Hebbian type synaptic plasticity, including LTP, LTD and spike timing-dependent plasticity,

and/or homeostatic plasticity depending on the stage of postnatal development to regulate their synaptic strengths and to select proper synaptic inputs.

ACKNOWLEDGEMENTS

I would like to express my sincere gratitude to Professor Masanobu Kano for having accepted me as a Ph-D student and for his supervision. I also warmly thank Professor Kouichi Hashimoto for his advices, supervision and helpful discussion. Finally I am very grateful to Drs. N. Uesaka, H. Nakayama and T. Mikuni for helpful advice for all experiments; Drs. K. Kitamura, T. Nakazawa, Y. Sugaya, G-M Good, E. S. K. Lai, T-H Kao, M. J. Choo and S. Inoue for helpful discussions; K. Matsuyama, M. Sekiguchi, A. Koseki, M. Tanaka, M. Watanabe and M. Yoshida for excellent technical assistance.

REFERENCES

Aiba, A., Kano, M., Chen, C., Stanton, M.E., Fox, G.D., Herrup, K., Zwingman, T.A., and Tonegawa, S. (1994). Deficient cerebellar long-term depression and impaired motor learning in mGluR1 mutant mice. Cell *79*, 377-388.

Bosman, L.W., Takechi, H., Hartmann, J., Eilers, J., and Konnerth, A. (2008). Homosynaptic long-term synaptic potentiation of the "winner" climbing fiber synapse in developing Purkinje cells. J Neurosci *28*, 798-807.

Carrillo, J., Nishiyama, N., and Nishiyama, H. (2013). Dendritic translocation establishes the winner in cerebellar climbing fiber synapse elimination. J Neurosci *33*, 7641-7653.

Hanawa, H., Kelly, P.F., Nathwani, A.C., Persons, D.A., Vandergriff, J.A., Hargrove, P., Vanin, E.F., and Nienhuis, A.W. (2002). Comparison of various envelope proteins for their ability to pseudotype lentiviral vectors and transduce primitive hematopoietic cells from human blood. Mol Ther *5*, 242-251.

Hansel, C., and Linden, D.J. (2000). Long-term depression of the cerebellar climbing fiber--Purkinje neuron synapse. Neuron *26*, 473-482.

Hartmann, J., Dragicevic, E., Adelsberger, H., Henning, H.A., Sumser, M., Abramowitz, J., Blum, R., Dietrich, A., Freichel, M., Flockerzi, V.*, et al.* (2008). TRPC3 channels are required for synaptic transmission and motor coordination. Neuron *59*, 392-398.

Hashimoto, K., Fukaya, M., Qiao, X., Sakimura, K., Watanabe, M., and Kano, M. (1999). Impairment of AMPA receptor function in cerebellar granule cells of ataxic mutant mouse stargazer. J Neurosci *19*, 6027-6036.

Hashimoto, K., Ichikawa, R., Kitamura, K., Watanabe, M., and Kano, M. (2009). Translocation of a "winner" climbing fiber to the Purkinje cell dendrite and subsequent elimination of "losers" from the soma in developing cerebellum. Neuron *63*, 106-118.

Hashimoto, K., and Kano, M. (2003). Functional differentiation of multiple climbing fiber inputs during synapse elimination in the developing

cerebellum. Neuron *38*, 785-796.

Hashimoto, K., and Kano, M. (2013). Synapse elimination in the developing cerebellum. Cell Mol Life Sci *70*, 4667-4680.

Hashimoto, K., Tsujita, M., Miyazaki, T., Kitamura, K., Yamazaki, M., Shin, H.S., Watanabe, M., Sakimura, K., and Kano, M. (2011). Postsynaptic P/Q-type Ca2+ channel in Purkinje cell mediates synaptic competition and elimination in developing cerebellum. Proc Natl Acad Sci U S A *108*, 9987-9992.

Hayama, T., Noguchi, J., Watanabe, S., Takahashi, N., Hayashi-Takagi, A., Ellis-Davies, G.C., Matsuzaki, M., and Kasai, H. (2013). GABA promotes the competitive selection of dendritic spines by controlling local Ca2+ signaling. Nat Neurosci *16*, 1409-1416.

Hensch, T.K. (2004). Critical period regulation. Annu Rev Neurosci *27*, 549-579.

Holtmaat, A., and Svoboda, K. (2009). Experience-dependent structural synaptic plasticity in the mammalian brain. Nat Rev Neurosci *10*, 647-658.

Ichikawa, R., Yamasaki, M., Miyazaki, T., Konno, K., Hashimoto, K., Tatsumi, H., Inoue, Y., Kano, M., and Watanabe, M. (2011). Developmental switching of perisomatic innervation from climbing fibers to basket cell fibers in cerebellar Purkinje cells. J Neurosci *31*, 16916-16927.

Ichise, T., Kano, M., Hashimoto, K., Yanagihara, D., Nakao, K., Shigemoto, R., Katsuki, M., and Aiba, A. (2000). mGluR1 in cerebellar Purkinje cells essential for long-term depression, synapse elimination, and motor coordination. Science *288*, 1832-1835.

Ito, M. (1984). The Cerebellum and Neural Control (New York, Raven Press).

Jackson, A.C., and Nicoll, R.A. (2011). The expanding social network of ionotropic glutamate receptors: TARPs and other transmembrane auxiliary subunits. Neuron *70*, 178-199.

Kakizawa, S., Yamasaki, M., Watanabe, M., and Kano, M. (2000). Critical period for activity-dependent synapse elimination in developing cerebellum.

J Neurosci *20*, 4954-4961.

Kano, M., and Hashimoto, K. (2009). Synapse elimination in the central nervous system. Curr Opin Neurobiol *19*, 154-161.

Kano, M., Hashimoto, K., Chen, C., Abeliovich, A., Aiba, A., Kurihara, H., Watanabe, M., Inoue, Y., and Tonegawa, S. (1995). Impaired synapse elimination during cerebellar development in PKC gamma mutant mice. Cell *83*, 1223-1231.

Kano, M., Hashimoto, K., Kurihara, H., Watanabe, M., Inoue, Y., Aiba, A., and Tonegawa, S. (1997). Persistent multiple climbing fiber innervation of cerebellar Purkinje cells in mice lacking mGluR1. Neuron *18*, 71-79.

Kano, M., Hashimoto, K., Watanabe, M., Kurihara, H., Offermanns, S., Jiang, H., Wu, Y., Jun, K., Shin, H.S., Inoue, Y.*, et al.* (1998). Phospholipase cbeta4 is specifically involved in climbing fiber synapse elimination in the developing cerebellum. Proc Natl Acad Sci U S A *95*, 15724-15729.

Katz, L.C., and Shatz, C.J. (1996). Synaptic activity and the construction of cortical circuits. Science *274*, 1133-1138.

Kawamura, Y., Nakayama, H., Hashimoto, K., Sakimura, K., Kitamura, K., and Kano, M. (2013). Spike timing-dependent selective strengthening of single climbing fibre inputs to Purkinje cells during cerebellar development. Nat Commun *4*, 2732.

Lichtman, J.W., and Colman, H. (2000). Synapse elimination and indelible memory. Neuron *25*, 269-278.

Llano, I., Marty, A., Armstrong, C.M., and Konnerth, A. (1991). Synaptic- and agonist-induced excitatory currents of Purkinje cells in rat cerebellar slices. J Physiol *434*, 183-213.

Luo, L., and O'Leary, D.D. (2005). Axon retraction and degeneration in development and disease. Annu Rev Neurosci *28*, 127-156.

Matsuzaki, M., Honkura, N., Ellis-Davies, G.C., and Kasai, H. (2004). Structural basis of long-term potentiation in single dendritic spines. Nature *429*, 761-766.

Menuz, K., and Nicoll, R.A. (2008). Loss of inhibitory neuron AMPA receptors contributes to ataxia and epilepsy in stargazer mice. J Neurosci *28*, 10599-10603.

Mikuni, T., Uesaka, N., Okuno, H., Hirai, H., Deisseroth, K., Bito, H., and Kano, M. (2013). Arc/Arg3.1 is a postsynaptic mediator of activity-dependent synapse elimination in the developing cerebellum. Neuron *78*, 1024-1035.

Mishina, M., and Sakimura, K. (2007). Conditional gene targeting on the pure C57BL/6 genetic background. Neurosci Res *58*, 105-112.

Mitsumura, K., Hosoi, N., Furuya, N., and Hirai, H. (2011). Disruption of metabotropic glutamate receptor signalling is a major defect at cerebellar parallel fibre-Purkinje cell synapses in staggerer mutant mice. J Physiol *589*, 3191-3209.

Miura, E., Fukaya, M., Sato, T., Sugihara, K., Asano, M., Yoshioka, K., and Watanabe, M. (2006). Expression and distribution of JNK/SAPK-associated scaffold protein JSAP1 in developing and adult mouse brain. J Neurochem *97*, 1431-1446.

Miyata, M., Finch, E.A., Khiroug, L., Hashimoto, K., Hayasaka, S., Oda, S.I., Inouye, M., Takagishi, Y., Augustine, G.J., and Kano, M. (2000). Local calcium release in dendritic spines required for long-term synaptic depression. Neuron *28*, 233-244.

Miyazaki, T., Fukaya, M., Shimizu, H., and Watanabe, M. (2003). Subtype switching of vesicular glutamate transporters at parallel fibre-Purkinje cell synapses in developing mouse cerebellum. Eur J Neurosci *17*, 2563-2572.

Miyazaki, T., and Watanabe, M. (2011). Development of an anatomical technique for visualizing the mode of climbing fiber innervation in Purkinje cells and its application to mutant mice lacking GluRdelta2 and Ca(v)2.1. Anat Sci Int *86*, 10-18.

Nakamura, M., Sato, K., Fukaya, M., Araishi, K., Aiba, A., Kano, M., and Watanabe, M. (2004). Signaling complex formation of phospholipase Cbeta4 with metabotropic glutamate receptor type 1alpha and 1,4,5-trisphosphate

receptor at the perisynapse and endoplasmic reticulum in the mouse brain. Eur J Neurosci *20*, 2929-2944.

Nakayama, H., Miyazaki, T., Kitamura, K., Hashimoto, K., Yanagawa, Y., Obata, K., Sakimura, K., Watanabe, M., and Kano, M. (2012). GABAergic inhibition regulates developmental synapse elimination in the cerebellum. Neuron *74*, 384-396.

Offermanns, S., Hashimoto, K., Watanabe, M., Sun, W., Kurihara, H., Thompson, R.F., Inoue, Y., Kano, M., and Simon, M.I. (1997). Impaired motor coordination and persistent multiple climbing fiber innervation of cerebellar Purkinje cells in mice lacking Galphaq. Proc Natl Acad Sci U S A *94*, 14089-14094.

Ohtsuki, G., and Hirano, T. (2008). Bidirectional plasticity at developing climbing fiber-Purkinje neuron synapses. Eur J Neurosci *28*, 2393-2400.

Palay, S., and Chan-Palay, V. (1974). Cerebellar Cortex (New York: Springer-Verlag).

Plath, N., Ohana, O., Dammermann, B., Errington, M.L., Schmitz, D., Gross, C., Mao, X., Engelsberg, A., Mahlke, C., Welzl, H.*, et al.* (2006). Arc/Arg3.1 is essential for the consolidation of synaptic plasticity and memories. Neuron *52*, 437-444.

Purves, D., and Lichtman, J.W. (1980). Elimination of synapses in the developing nervous system. Science *210*, 153-157.

Sawada, Y., Kajiwara, G., Iizuka, A., Takayama, K., Shuvaev, A.N., Koyama, C., and Hirai, H. (2010). High transgene expression by lentiviral vectors causes maldevelopment of Purkinje cells in vivo. Cerebellum *9*, 291-302.

Smith-Hicks, C., Xiao, B., Deng, R., Ji, Y., Zhao, X., Shepherd, J.D., Posern, G., Kuhl, D., Huganir, R.L., Ginty, D.D.*, et al.* (2010). SRF binding to SRE 6.9 in the Arc promoter is essential for LTD in cultured Purkinje cells. Nat Neurosci *13*, 1082-1089.

Takagishi, Y., Hashimoto, K., Kayahara, T., Watanabe, M., Otsuka, H., Mizoguchi, A., Kano, M., and Murata, Y. (2007). Diminished climbing fiber

innervation of Purkinje cells in the cerebellum of myosin Va mutant mice and rats. Dev Neurobiol *67*, 909-923.

Tanaka, J., Nakagawa, S., Kushiya, E., Yamasaki, M., Fukaya, M., Iwanaga, T., Simon, M.I., Sakimura, K., Kano, M., and Watanabe, M. (2000). Gq protein alpha subunits Galphaq and Galpha11 are localized at postsynaptic extra-junctional membrane of cerebellar Purkinje cells and hippocampal pyramidal cells. Eur J Neurosci *12*, 781-792.

Torashima, T., Okoyama, S., Nishizaki, T., and Hirai, H. (2006). In vivo transduction of murine cerebellar Purkinje cells by HIV-derived lentiviral vectors. Brain Res *1082*, 11-22.

Turrigiano, G. (2012). Homeostatic synaptic plasticity: local and global mechanisms for stabilizing neuronal function. Cold Spring Harb Perspect Biol *4*, a005736.

Turrigiano, G.G. (2008). The self-tuning neuron: synaptic scaling of excitatory synapses. Cell *135*, 422-435.

Uesaka, N., Mikuni, T., Hashimoto, K., Hirai, H., Sakimura, K., and Kano, M. (2012). Organotypic coculture preparation for the study of developmental synapse elimination in mammalian brain. J Neurosci *32*, 11657-11670.

Watanabe, M., and Kano, M. (2011). Climbing fiber synapse elimination in cerebellar Purkinje cells. Eur J Neurosci *34*, 1697-1710.

Yamasaki, M., Miyazaki, T., Azechi, H., Abe, M., Natsume, R., Hagiwara, T., Aiba, A., Mishina, M., Sakimura, K., and Watanabe, M. (2011). Glutamate receptor delta2 is essential for input pathway-dependent regulation of synaptic AMPAR contents in cerebellar Purkinje cells. J Neurosci *31*, 3362-3374.

Yamazaki, M., Fukaya, M., Hashimoto, K., Yamasaki, M., Tsujita, M., Itakura, M., Abe, M., Natsume, R., Takahashi, M., Kano, M.*, et al.* (2010). TARPs gamma-2 and gamma-7 are essential for AMPA receptor expression in the cerebellum. Eur J Neurosci *31*, 2204-2220.

Yoshida, T., Fukaya, M., Uchigashima, M., Miura, E., Kamiya, H., Kano, M.,

and Watanabe, M. (2006). Localization of diacylglycerol lipase-alpha around postsynaptic spine suggests close proximity between production site of an endocannabinoid, 2-arachidonoyl-glycerol, and presynaptic cannabinoid CB1 receptor. J Neurosci *26*, 4740-4751.